ONLINE FIRST

This is a provisional PDF only. Copyedited and fully formatted version will be made available soon.

REPORTS OF PRACTICAL ONCOLOGY AND RADIOTHERAPY

ISSN: 1507-1367

e-ISSN: 2083-4640

TMPO-AS1-hsa-let-7b-5p-EZH2-RNA network predicts poor survival in basal-like breast cancer patients

Authors: Prerna Vats, Bhavika Baweja, Sakshi Nirmal, Aditi Singh, Rajeev Nema

DOI: 10.5603/rpor.105252

Article type: Research paper

Published online: 2025-03-19

This article has been peer reviewed and published immediately upon acceptance.
It is an open access article, which means that it can be downloaded, printed, and distributed freely,
provided the work is properly cited.

TMPO-AS1-hsa-let-7b-5p-EZH2-RNA network predicts poor survival in basal-like breast cancer patients

DOI: 10.5603/rpor.105252

Prerna Vats, Bhavika Baweja, Sakshi Nirmal, Aditi Singh, Rajeev Nema

Department of Biosciences, Manipal University Jaipur, Dehmi Kalan, Jaipur-Ajmer Expressway, Jaipur, Rajasthan, India

Address for Correspondence: Dr Rajeev Nema, Assistant Professor
Department of Biosciences, Manipal University Jaipur, Dehmi Kalan, Jaipur-Ajmer Expressway, Jaipur, Rajasthan, 303007, India; e-mail: rajeev.nema@jaipur.manipal.edu

Abstract

Background: The study explores the role of non-coding ribonucleic acids (RNAs) and higher enhancer of zeste homolog 2 (EZH2) gene in breast cancer progression, examining how micro RNA (miRNA) and long noncoding RNA (lncRNA) control EZH2, potentially influencing oncogene growth and treatment failure.

Materials and methods: The databases used in the study included Cyclebase 3.0 and CellTracer to determine EZH2's role in cell cycle, Oncomine, OncoMX and The University of Alabama At Birmingham Cancer Data Analysis Portal (UALCAN) for Pan-cancer analysis, The Cancer Genomic Atlas Portal (TCGA Portal), Gene Expression Profiling Interactive Analysis (GEPIA2), OncoDB, CR2Cancer, Encyclopaedia of RNA Interactomes (ENCORI), and The Cancer Genome Altas Analyzer (TCGAnalyzeR v1.0) for differential expression analysis, CR2Cancer, OncoDB, MethMarkerDB, and Wanderer databases for epigenetic alteration analysis, Kaplan-Meier Plotter for survival analysis, Breast Cancer Gene Expression Miner (bc-GenExMiner v5.0) for hormone receptor analysis, Tumor-Immune System Interaction Database (TISIDB), Cancer Single Cell State Atlas (CancerSEA), TNMplot, DriverDBv4, and ENCORI for biological

processes, cell cycle checkpoints and metastasis analysis, Enrichr, Tumor Immune Estimation Resource (TIMER 2.0), Gepia2 for transcription factor analysis, miRNet, Transcriptome Alterations in Cancer Omnibus (TACCO), and CancerMIRome for miRNA analysis, Enrichr, UALCAN, and ENCORI for lncRNA analysis.

Results: The EZH2 gene is overexpressed in breast cancer (BRCA) tumors, metastatic tissues, and circulating tumor cells, potentially leading to cancer progression. Patients with high EZH2 expression have shorter overall survival (OS), distant metastasis-free survival (DMFS), and relapse-free survival (RFS) compared to those with low expression. Estrogen receptot (ER)-negative BRCA tumors and PR-negative tumors have EZH2 gene and eucariotic transcription factor (E2F2) levels. The EZH2/E2F2 axis may assist ER/PR-negative BRCA by sponging homosapiens microRNA family (hsa-let-7b-5p) through lncRNA-thymopoietin antisense transcript 1 (TMPO-AS1). Overexpression of the EZH2 protein is associated with BRCA metastasis.

Conclusion: EZH2 overexpression in basal-like BRCA is mediated by a competing endogenous RNA (ceRNA) network and regulating their expression levels may facilitate better survival outcomes.

Keywords: breast cancer; ceRNA network; EZH2; Kaplan-Meier Plotter; prognosis

Introduction

Breast cancer is a global disease with the highest incidence rate among all cancers. In 2020, it had an estimated 2.3 million new cases, representing 11.7% of all new cancers [1]. Prognostic and predictive factors for future recurrence or death from breast cancer include patient age, comorbidity, tumor size, tumor grade, number of involved axillary lymph nodes and, possibly, a biomarker status [2, 3]. Algorithms have been published to estimate recurrence rates, and a validated computer-based model (Adjuvant! Online for breast cancer) is available to estimate 10-year disease-free survival [4]. Breast cancer detection and intervention in the early stages are key to improving prognoses and reducing mortality rates. Researchers have used various diagnostic approaches, including mammography, magnetic resonance imaging, ultrasound, biopsies, serum screening for micro ribonucleic acid (miRNAs), blood-based proteomics, biomarker analysis, and biosensor technologies [5]. Comprehensive treatment primarily involves surgery combined with chemotherapy, endocrine therapy, radiation therapy, and targeted therapies [6, 7]. New

gene-expression profiling studies have found four different types of breast cancer: the basal-like type, the human epidermal growth factor receptor 2 (HER2)-negative type, and the two luminal estrogen receptor (ER)-positive types, which have been named luminal A and luminal B [8]. These newly defined molecular subgroups have distinct clinical outcomes. Gene-expression profiling technology aims to provide better predictions of clinical outcomes than traditional clinical and pathological parameters [9].

Studies have shown that enhancer of zeste homolog 2 (EZH2) is frequently overexpressed in breast cancer cells, silencing tumor suppressor genes and promoting tumor cell growth and poor survival [10]. Targeting a competing endogenous miRNA–long noncoding RNA (lncRNA)–EZH2-RNA network could be an effective strategy for treating breast cancer. High levels of EZH2 expression are associated with a poorer prognosis for several types of cancer, including breast cancer [11], prostate cancer [12], and bladder cancer [13]. In breast cancer, patients with high EZH2 expression have a higher risk of recurrence and shorter overall survival. Clinical trials are developing and testing new drugs targeting EZH2, providing a fresh approach to cancer treatment [14–16]. This study of the miRNA-lncRNA-EZH2-RNA network and its function in breast cancer will lead to the development of novel medicines that will improve the prognosis for individuals suffering from this dreadful illness. This article focuses on the role of hypomethylation in cancer development, particularly human breast cancer. It investigates how miRNA, lncRNA, and gene overexpression of EZH2 impact oncogene development and resistance to treatment.

Materials and methods

Expression analysis of EZH2

For this study, we used Cyclebase 3.0 [17], CellTracer [18], Oncomine [19], OncoMX [20] and The University of Alabama At Birmingham Cancer Data Analysis Portal (UALCAN) [21] to assess EZH2 expression levels in the cell cycle and in tumor tissue *vs.* normal tissues across pan-cancer. The study examined how EZH2 mRNA expression differed in breast cancer (BRCA) *vs.* normal samples. It was achieved by utilizing databases such as UALCAN, The Cancer Genomic Atlas Portal (TCGA Portal) [22], Gene Expression Profiling Interactive Analysis (GEPIA2) [23], OncoDB [24], CR2Cancer [25], Encyclopaedia of RNA Interactomes (ENCORI) [26], and The Cancer Genome Altas Analyzer (TCGAnalyzer v1.0) [27]. We analyzed the methylation status of

EZH2 in BRCA using the UALCAN, CR2Cancer, OncoDB, MethMarkerDB [28], and TCGA Wanderer [29] databases. The study used Breast Cancer Gene-Expression Miner v5.0 [30] to look at the connection between EZH2 expression levels and the patients' clinical and pathological features, such as their estrogen, progesterone receptor status, and UALCAN and Tumor-Immune System Interaction Database (TISIDB) [31] databases for BRCA subtypes and expression of EZH2 based on patient's age analysis. Using Cancer Single Cell State Atlas (CancerSEA) [32], we investigated the association of EZH2 with BRCA's biological process. ENCORI database was used to determine the correlation between EZH2 and Cyclin-CDKs checkpoints. The metastatic analysis was carried out using TNMplot [33] and DriverDBv4 [34].

The survival analysis of EZH2 and its transcription factors

The study used the BRCA datasets and the Kaplan-Meier Plotter [35] to look at relapse-free survival (RFS), overall survival (OS), distant metastasis-free survival (DMFS), and **PPS [PFS?]**. It did this by dividing patients by median and looking at the results. The screening conditions were as follows: "Cancer: BRCA"; "Gene symbol: EZH2"; Affy id: 203358_s_at. Using the Enrichr [36] database, we examined transcriptional factors involved in tissue-specific gene expression regulation. The study also analyzed the correlation between the eukaryotic transcription factor (E2F) family and the EZH2 gene using the ENCORI, Tumor Immune Estimation Resource (TIMER) [37], OncoDB, and GEPIA2 databases.

An analysis of non-coding-related regulatory networks

The study analyzed the miRNA network associated with EZH2 using the miRNet [38] database. We verified the correlation between EZH2 and miRNA using the ENCORI, Transcriptome Alterations in Cancer Omnibus (TACCO) [39], and CancerMIRNome [40] databases. We used the CancerMIRNome, Kaplan-Meier (KM) plotter, and ENCORI to figure out what the EZH2-associated miRNA meant for prognosis. The CancerMIRome and UALCAN were used to look at differences in miRNA expression based on normal vs. tumor expression. We used the Enrichr and UALCAN databases to identify the lncRNA associated with EZH2. Using the ENCORI, GEPIA2, OncoDB, and miRNet databases, we confirmed the co-relationship between EZH2 and specific lncRNA. We also determined individual lncRNA expression using UALCAN and OncoDB.

A molecular mechanism analysis of EZH2

The study validated the relationship between a gene and ESR1, PGR, using the ENCORI, OncoDB, and Breast Cancer Gene Expression Miner (bc-GenExMiner v5.0) databases. It also identified a correlation between the competing endogenous RNA (ceRNA) network and ESR1 and PGR, including E2F2, homosapiens microRNA family (hsa-let-7b-5p), and thymopoietin antisense transcript 1 (TMPO-AS1).

Statistical analysis

The study analyzed EZH2 gene expression differences between tumor and normal tissues, using log-rank tests to compare survival, performance heterogeneity, and gene enrichment, with statistical significance at $p < 0.05$. We analyzed the validity of the data using statistical methods based on online databases.

Results

EZH2 expression levels in pan-cancer and breast cancer

To find out what role EZH2 plays in the cell cycle and cancer progression, we first used Cyclebase 3.0 to examine EZH2 expression in the phases of cell cycle. As shown in Figure 1A, EZH2's peak time is in the S phase. Next, we used the CellTracer database, which provided extensive insights into the impact of various relationships on cell development pathways and served as a foundation for identifying biomarkers and investigating novel treatments within the tumor environment. We found that EZH2 is significantly associated with quiescence, invasion, and hypoxia, which are some of the crucial hallmarks of cancer, but its expression is not involved in apoptosis, which helps in breast cancer progression, as shown in Figure 1B. The TISIDB database was also used to identify the role of EZH2 in various biological processes, molecular functions, cellular components, KEGG, and reactomes, as listed in Supplementary File — Table S1. Using the Oncomine and OncoMX databases, we were able to show that all TCGA tumors had the heightened levels of EZH2. The levels were higher in tumor tissue than in normal tissue (Fig. 1C and Supplementary File — Tab. S2). In addition, we validated the pan-cancer view using the UALCAN database, and we found the same results as mentioned above, as shown in Figure 1D. The above-mentioned results strongly indicate the oncogenic properties of EZH2

and hence its role in tumor progression. Next, statistical analysis revealed a high expression of EZH2 in breast cancer compared to the healthy group. This difference was statistically significant ($p < 0.05$), as shown in Figures 2A–F. The databases used were UALCAN, TCGA Portal, GEPIA2, oncoDB, CR2Cancer, and ENCORI. Transcriptomic analysis was also carried out in breast invasive carcinoma cells using TCGAnalyzeR v1.0, as shown in Figure 2G, and the data showed upregulation in the EZH2 expression level in BRCA with a log-fold change of 2.08. We linked the amount of methylation in the promoter region to tumor formation. As a result, we investigated EZH2 promoter methylation in pan-can using the CR2Cancer database (Supplementary File — Tab. S3) and found a strong association of EZH2 methylation with breast cancer tissues as compared to other TCGA cancers, ($R = –0.277$, $p = 1.27e–16$). The negative correlation value indicated towards the hypomethylation status of EZH2. Further, the databases used to analyze the methylation profile were UALCAN, CR2Cancer, OncoDB, and MethMarkerDB, respectively. Figure 3A–E reveals that the EZH2 promoter methylation level in breast cancer was much lower than in normal tissues, indicating hypomethylation. The findings indicate a connection between the degree of methylation in the promoter region and EZH2 expression, which, in turn, influences the survival status of breast cancer patients. Also, Wanderer, an interactive tool to explore deoxyribonucleic acid (DNA) methylation and gene expression data in human cancer, was used to compare the methylation status of EZH2 in a ($n = 30$) normal sample *vs.* ($n = 30$) BRCA tumor, and the results showed hypomethylation in breast invasive carcinoma patients, as shown in Supplementary File — Figure 1A–C.

EZH2 expression level survival analysis in breast cancer

The KM Plotter online database provided the dataset from which we analyzed the EZH2 gene in 4,929 patients. In the 120-month study, higher levels of EZH2 transcripts were linked to worsening RFS, OS, DMFS, and PPS for all breast cancer patients. These were RFS [hazard ratio (HR) = 1.5, confidence interval (CI) = 136–167, $p = 6.2e–15$], OS (HR = 1.31, CI = 1.08–158, $p = 0.0063$), DMFS (HR = 1.45, CI = 1.24–1.07, $p = 3.9e\text{-}6$), and PPS (HR = 1.47, CI = 1.16–186, $p = 0.0012$), as shown in Figure 4A–D. Also, as listed in Supplementary File — Table S4, the difference between the high expression cohort and low expression cohort suggests that targeting and inhibiting the levels of EZH2 in BRCA patients can significantly result in good prognosis improving the survival outcomes. By using gold standards like marker of proliferation

Ki-67 (MKI67), ESR1, and HER2 biomarkers, we looked more closely at the EZH2 expression multivariate analysis and found a strong link between it and these markers, as shown in Figure 4E (HR = 1.5, CI = 1.36–1.67, P = 6.2e–15). We concluded from this overall analysis that there is a significant correlation between EZH2 gene expression and the poor prognosis of breast cancer.

EZH2 expression with ER and PR receptors and breast cancer subclass

We also aimed to confirm the association between EZH2 expression and Estrogen-Progesterone receptors using Breast Cancer Gene-Expression Miner v5.0. Our findings revealed an overexpression level of ER and PR negative hormone receptors, as depicted in Figure 5A–C. This suggests a strong correlation between EZH2 expression and ER/PR negative breast cancer. We were very curious about EZH2's role in the breast cancer subclass following the validation gene expression and correlation study findings. Using three distinct databases, namely bc-GenExMiner v5.0, UALCAN, and TISIDB, our analysis revealed a significant enhancement of EZH2 in triple negative breast cancer (TNBC) and basal subclasses, as illustrated in Figure 5D–G. Also, by using the bc-GenExMiner v5.0 TCGA RNA seq dataset, we identified the expression level of EZH2 in healthy, tumor-adjacent, non-basal-like and non-TNBC, and basal-like and TNBC, and, interestingly, the results showed the highest expression of EZH2 in Basal-like and TNBC as compared to others, suggesting an important role of EZH2 in aggressive tumors as shown in Figure 5H. After this study, we used the ENCORI database to look at the EZH2 gene in relation to the ESR1 and PGR genes. To our surprise, we discovered that the EZH2 gene had a strong negative correlation with the ESR1 (R = –0.425, p = 1.01e–49) and PGR (R = –0.399, p = 1.59e–43) genes. Figure S2A–B (Supplementary File) demonstrates a close link between EZH2 overexpression and aggressive types of breast cancer. Further, we analyzed EZH2’s expression based on patient’s age group and the results revealed that overexpression of EZH2 is more aggressive at a younger age as compared to the older patients as shown in Figure 5I.

EZH2 metastasis and biological processes involvements

We also analyzed EZH2 in relation to various cellular biology processes and found a significant positive correlation between EZH2 and the cell cycle (0.56), DNA repair (0.49), DNA damage (0.43), and cell proliferation (0.36), with a p-value of less than 0.05, as illustrated in Figure 6A–

E. As established earlier, EZH2 plays an important role in cancer progression, which aligns with our analysis of cell cycle checkpoints as listed in Supplementary File — Table S5. EZH2 showed a strong positive correlation with Cyclin E1/CDK2 (R = 0.67 and 0.57, respectively) and Cyclin B1/CDK1 (R = 0.67 and 0.69, respectively), key regulators of the S and M phases of the cell cycle. Whereas, the weaker correlation between G0/G1 and G2 phases checkpoints reflect a more specialized function of EZH2 in cell division and tumor progression. After that, we did a metastasis analysis with the TNMplot database to examine the connections between the EZH2 genes, and we found significant metastasis with gene chip (p = 1.58 e–28, as shown in Figure 6F) and with RNA-Seq (p = 5.01 e–53, as shown in Figure 6G), and the data was later corroborated with DriverDBv4 databases, revealing a considerably increased level of EZH2 in the metastatic phase, as seen in Figure 6H.

EZH2 transcriptional regulation in BRCA

Cancer cells highly depend on the constitutive expression of transcriptional factors (TFs) to support their growth and survival. Increasing knowledge of the TFs' mechanisms of action and regulatory networks has led to a better understanding of their roles in cancer and other diseases. Given the critical role TFs play in cancer, researchers have made significant efforts to develop drugs that target TFs. Several drugs targeting TFs in cancer are currently in different phases of clinical trials. We used the Enrichr database (Supplementary File — Table S6) to identify transcriptional factors associated with EZH2, as well as the ENCORI database to identify correlations. We then chose eight transcriptional factors from the E2F family, including E2F1, E2F2, E2F3, E2F4, E2F5, E2F6, E2F7, and E2F8, as shown in Figure 7 A–D and Supplementary File — Figure S2 C–F, and found that out of those eight, only four transcriptional factors (E2F1, E2F2, E2F7, and E2F8) have the highest correlation value with EZH2, which states that the activity or expression level of the transcription factor is closely related to the activity or expression level of the EZH2 gene. To validate it further, we used three different databases, such as TIMER, OncoDB, and the GEPIA database, as shown in Figure 7 E-P. After this study, we used the ENCORI database to look at the E2F1, E2F2, E2F7, and E2F8 genes in relation to the ESR1 and PGR genes. To our surprise, we discovered that the E2F2 gene had the highest negative correlation with the ESR1 and PGR genes (–0.409 and –0.395, respectively). The

Supplementary File — Figure S3A–H demonstrates a close link between E2F1, E2F2, E2F7, and E2F8 overexpression and aggressive types of breast cancer.

EZH2-non-coding RNA regulatory network

The mechanism for BRCA's EZH2 overexpression is unclear. Supplementary File — Figure S4A shows the top 24 miRNAs associated with EZH2 identified by the miRNet database, a platform for visualizing miRNA networks. Further study using the ENCORI database revealed that only 7 miRNAs (hsa-let-7b-5p, hsa-mir-26a-5p, hsa-mir-101-3p, hsa-mir-214-3p, hsa-mir-217, hsa-mir-1-3p, and hsa-miR-101-3p) out of 24 miRNAs exhibited a negative correlation with EZH2 gene expression, as presented in Table 1. The table also showed that hsa-let-7b-5p has the best negative correlation (R = –0.289) with EZH2 in BRCA patients. To ensure the reliability of our findings, we utilized the TACCO, CancerMIRNome, and ENCORI databases. And we found that EZH2 and hsa-let-7b-5p negatively correlated with each other, as shown in Figure 8A–C. Next, we analyzed the hsa-let-7b-5p expression in BRCA patients compared to normal by using the CancerMIRNome database, and we found that hsa-let-7b-5p was downregulated in BRCA patients as compared with normal, as shown in Figure 8D. This down-expression was further validated by using the UALCAN database, and we found similar results as shown in Figure 8E. Survival analysis of hsa-let-7b-5p in BRCA patients using the CancerMIRNome (HR = 0.58, CI = 0.42–0.80, p = 8.37e–04), KM plotter (HR = 0.68, CI = 0.56-0.83, p = 0.00014), and ENCORI (HR = 0.56, p = 0.00038) databases showed that the downregulation of hsa-let-7b-5p is associated with poor prognosis, as shown in Supplementary File — Figure S4B–D. Also, the correlation analysis of hsa-let-7b-5p with ESR1 and PGR genes using the ENCORI database (Supplementary File — Figure S4E–F) showed a significant relationship between hsa-let-7b-5p *vs.* ESR1 (R = 0.267, p = 3.60e–19) and hsa-let-7b-5p vs. PGR (R = 0.274, p = 3.64e–20), indicating a positive association with the expression of hsa-let-7b-5p and ESR1/PGR genes. This study also investigates how EZH2, miRNAs, and lncRNAs work together. Using the Enrichr database, we discovered several lncRNAs linked to EZH2. The lncRNAs shown in Supplementary File — Table S7 are TMPO-AS1, PRC1-AS1, RRM1-AS1, H2AZ1-DT, LINC01775, SGO1-AS1, DEPDC1-AS1, HMMR-AS1, UBL7-AS1, and APOBEC3B-AS1. We checked how each lncRNA was expressed in the case of BRCA using UALCAN and found that 4 out of 10 lncRNAs were significantly upregulated, as shown in Supplementary File — Table S8.

Further, we correlated these lncRNAs to EZH2 in the BRCA using ENCORI as shown in Table 2 and found that TMPO-AS1 was strongly positively correlated with EZH2 (R = 0.587, P = 4.16e–103, shown in Figure 8F) as compared to others. Further validation of the data was done using the GEPIA2, and OncoDB databases, Figures 8G–H show that TMPO-AS1 had the strongest positive correlation (R = 0.45, R = 0.5014 respectively) with EZH2. We also found that TMPO-AS1 is significantly overexpressed in BRCA patients compared to normal. We used the UALCAN and OncoDB databases, as shown in Figure 8 I–J. Further correlation between E2F2 *vs.* TMPO-AS1 showed a strong positive correlation between both, with an R value of 0.561 and a P value of 1.46e-92. However, on analyzing the correlation between hsa-let-7b-5p and TMPO-AS1, a negative correlation was observed (R = –0.204, p = 1.12e–11). It shows that TMPO-AS1 has a sponge effect on hsa-let-7b-5p because lncRNAs are stable and can regulate miRNA expression. Very interestingly, TMPO-AS1 *vs.* ESR1 (R = –0.167, p = 2.41e–08) and TMPO-AS1 *vs.* PGR (R = –0.232, p = 5.52e–15) also showed a negative correlation, indicating the role of TMPO-AS1 in tumor aggression. The results are shown in Supplementary File — Figure S5 A–D. Also, a network created using the miRNet database between mRNA-miRNA-lncRNA shows direct interaction between EZH2-hsa-let-7b-5p-TMPO-AS1, as shown in Supplementary File — Figure S5E.

Discussion

EZH2, an essential gene involved in breast cancer development and progression, regulates gene expression and chromatin structure. Understanding EZH2's role could lead to the development of targeted therapies that improve treatment options for patients. Preclinical studies have demonstrated the potential of EZH2 inhibitors for targeting and inhibiting EZH2, a protein frequently overexpressed in breast cancer cells [42, 43]. As listed in Supplementary Table 9 and 10, retrieved from GSCA database, showed that there are various positively and negatively correlated drugs associated with EZH2’s overexpression. The positive correlation between the gene and the drug could lead to drug resistance, whereas the negative correlation could make the drug sensitive. Challenges in targeting EZH2 as a therapy include potential resistance mechanisms, the need to identify biomarkers for patient response, and long-term effects on normal cells and tissues. Small molecular inhibitors or gene knockdowns inhibit EZH2, which reduces cancer cell growth and tumor formation. Recent studies suggest targeting histone

methylation as a promising approach for cancer therapy. A bioinformatic study of 2,000 breast cancer patients showed that EZH2 HMT is a major epigenetic driver of TNBC progression. Patients with TNBC had higher levels of EZH2 expression than patients who did not have TNBC [44]. Screening predictive biomarkers, such as EZH2 mutation or overexpression, is important for personalized, precision therapy. Combining EZH2 inhibitors with other treatments is critical, as preclinical studies have shown that EZH2 inhibitors combined with immunotherapy or chemotherapy have a synergistic effect.

The study reveals that EZH2's peak time is in the S phase and is associated with quiescence, invasion, and hypoxia in breast cancer progression. Previous study has shown EZH2 to be a key component of the polycomb repressive complex 2 (PRC2), and is known to methylate histone H3 on lysine 27 (H3K27me3), leading to gene silencing, and this epigenetic modification is crucial for regulating the expression of various cell cycle checkpoints involved in cell cycle progression [45–47]. For example, Tazemetostat is a Food and Drug administration (FDA)-approved drug acting as an EZH2 methyltransferase inhibitor, working on the same mechanism. Targeting EZh2’s role in cell proliferation can be approached by disrupting its interaction with key cell cycle regulators. The study found a strong positive association between EZH2 and Cyclin/CDKs, suggesting that EZH2 promotes the G1/S transition, leading to DNA replication, and inhibiting it may cause cell cycle arrest in the G1 phase. Additionally, EZH2 is crucial for the G2/M transition, preventing cancer cells from entering mitosis and reducing tumor cell proliferation. This study also revealed that EZH2 DNA hypomethylation, the first epigenetic abnormality found in human tumors, is the first study to suggest such data in BRCA. During the development of cancer, DNA demethylation may involve hemimethylated dyads as bridges, and then the loss of methylation spreads to both strands. The study linked higher levels of EZH2 transcripts to worse RFS, OS, DMFS, and PPS for all breast cancer patients. The study found a strong link between EZH2 and the transcription factor E2F2, which promotes breast cancer by increasing gene expression that promotes cell proliferation and survival while suppressing genes that inhibit these processes. Cancer controls EZH2 gene expression, leading to aggressive tumor growth. Targeting EZH2 in breast cancer treatment holds enormous promise as a potential therapeutic strategy. The study also found that only seven out of 24 miRNAs had a negative correlation with EZH2 gene expression. In BRCA patients, hsa-let-7b-5p had the strongest negative correlation with EZH2. BRCA patients significantly overexpressed TMPO-AS1, which had the strongest

positive correlation with EZH2. Further research should explore the potential clinical applications of manipulating EZH2 regulation in cancer treatment. Targeted therapies focusing on the molecular causes of prostate cancer, ovarian cancer, and lung cancer, all linked to abnormal EZH2 expression, could potentially treat these diseases.

Conclusion

The study links the hsa-let-7b-5p-TMPO-AS1-EZH2 Mediated Network, a key epigenetic modulator in TNBC subtypes, to poor overall survival. When analyzed at the molecular level, EZH2 showed that metastasis spreads faster. Understanding subtype-specific regulation is crucial for developing targeted therapies and personalized treatment approaches. It's possible that blocking TMPO-AS1-EZH2 could lead to the development of TMPO-AS1-EZH2 as a targeted treatment for metastases from TNBC.

Funding

None declared.

Conflicts of interest

The authors declare that they have no competing interests.

Author contribution

R.N.: conception, study design, critical reading, and intellectual assessment of the manuscript, study design, and preparation of the manuscript. PV: study design, and preparation of the manuscript. BB: critical reading. SN: critical reading. AS: study design, and preparation of the manuscript.

Data availability

The data for this in-silico study were sourced from publicly accessible databases. The respective links and references for these datasets are provided in the methodology section for transparency and reproducibility.

Ethical clearance

Since this study exclusively utilized publicly available online databases for data extraction and analysis, ethical approval was not necessary for the preparation of this article.

References

1. Sung H, Ferlay J, Siegel RL, et al. Global Cancer Statistics 2020: GLOBOCAN Estimates of Incidence and Mortality Worldwide for 36 Cancers in 185 Countries. CA Cancer J Clin. 2021; 71(3): 209–249, doi: 10.3322/caac.21660, indexed in Pubmed: 33538338.
2. Yang R, Wu Y, Qi Y, et al. A nomogram for predicting breast cancer specific survival in elderly patients with breast cancer: a SEER population-based analysis. BMC Geriatr. 2023; 23(1): 594, doi: 10.1186/s12877-023-04280-8, indexed in Pubmed: 37749538.
3. Castellarnau-Visús M, Soveral I, Regueiro Espín P, et al. Prognostic factors in Luminal B-like HER2-negative breast cancer tumors. Surg Oncol. 2023; 49: 101968, doi: 10.1016/j.suronc.2023.101968, indexed in Pubmed: 37364335.
4. Campbell HE, Gray AM, Harris AL, et al. Estimation and external validation of a new prognostic model for predicting recurrence-free survival for early breast cancer patients in the UK. Br J Cancer. 2010; 103(6): 776–786, doi: 10.1038/sj.bjc.6605863, indexed in Pubmed: 20823886.
5. Abdul Wahab MR, Palaniyandi T, Viswanathan S, et al. Biomarker-specific biosensors revolutionise breast cancer diagnosis. Clin Chim Acta. 2024; 555: 117792, doi: 10.1016/j.cca.2024.117792, indexed in Pubmed: 38266968.
6. Liu Z, Li J, Zhao F, et al. Long-term survival after neoadjuvant therapy for triple-negative breast cancer under different treatment regimens: a systematic review and network meta-analysis. BMC Cancer. 2024; 24(1): 440, doi: 10.1186/s12885-024-12222-9, indexed in Pubmed: 38594636.
7. Dailah HG, Hommdi AA, Koriri MD, et al. Potential role of immunotherapy and targeted therapy in the treatment of cancer: A contemporary nursing practice. Heliyon. 2024; 10(2): e24559, doi: 10.1016/j.heliyon.2024.e24559, indexed in Pubmed: 38298714.
8. Rakha EA, Pareja FG. New Advances in Molecular Breast Cancer Pathology. Semin Cancer Biol. 2021; 72: 102–113, doi: 10.1016/j.semcancer.2020.03.014, indexed in Pubmed: 32259641.
9. Varnier R, Sajous C, de Talhouet S, et al. Using Breast Cancer Gene Expression Signatures in Clinical Practice: Unsolved Issues, Ongoing Trials and Future Perspectives. Cancers (Basel). 2021; 13(19), doi: 10.3390/cancers13194840, indexed in Pubmed: 34638325.

10. Chen Y, Zhu H, Luo Yi, et al. EZH2: The roles in targeted therapy and mechanisms of resistance in breast cancer. Biomed Pharmacother. 2024; 175: 116624, doi: 10.1016/j.biopha.2024.116624, indexed in Pubmed: 38670045.
11. Yu F, Li L, Zhang M, et al. Phosphorylation of EZH2 differs HER2-positive breast cancer invasiveness in a site-specific manner. BMC Cancer. 2023; 23(1): 948, doi: 10.1186/s12885-023-11450-9, indexed in Pubmed: 37803297.
12. Yang Y, Fan H, Liu H, et al. NOP2 facilitates EZH2-mediated epithelial-mesenchymal transition by enhancing EZH2 mRNA stability via m5C methylation in lung cancer progression. Cell Death Dis. 2024; 15(7): 506, doi: 10.1038/s41419-024-06899-w, indexed in Pubmed: 39013911.
13. Li F, Wang P, Ye J, et al. Serum EZH2 is a novel biomarker for bladder cancer diagnosis and prognosis. Front Oncol. 2024; 14: 1303918, doi: 10.3389/fonc.2024.1303918, indexed in Pubmed: 38476362.
14. Freitag T, Kaps P, Ramtke J, et al. Combined inhibition of EZH2 and CDK4/6 perturbs endoplasmic reticulum-mitochondrial homeostasis and increases antitumor activity against glioblastoma. NPJ Precis Oncol. 2024; 8(1): 156, doi: 10.1038/s41698-024-00653-3, indexed in Pubmed: 39054369.
15. Ozgun G, Yaras T, Akman B, et al. Retinoids and EZH2 inhibitors cooperate to orchestrate anti-oncogenic effects on bladder cancer cells. Cancer Gene Ther. 2024; 31(4): 537–551, doi: 10.1038/s41417-024-00725-3, indexed in Pubmed: 38233533.
16. Zhang Q, Shi Y, Liu S, et al. EZH2/G9a interact to mediate drug resistance in non-small-cell lung cancer by regulating the SMAD4/ERK/c-Myc signaling axis. Cell Rep. 2024; 43(2): 113714, doi: 10.1016/j.celrep.2024.113714, indexed in Pubmed: 38306271.
17. Santos A, Wernersson R, Jensen LJ. Cyclebase 3.0: a multi-organism database on cell-cycle regulation and phenotypes. Nucleic Acids Res. 2015; 43(Database issue): D1140–D1144, doi: 10.1093/nar/gku1092, indexed in Pubmed: 25378319.
18. Guo Q, Wang P, Liu Q, et al. CellTracer: a comprehensive database to dissect the causative multilevel interplay contributing to cell development trajectories. Nucleic Acids Res. 2023; 51(D1): D861–D869, doi: 10.1093/nar/gkac892, indexed in Pubmed: 36243976.

19. Rhodes DR, Yu J, Shanker K, et al. ONCOMINE: a cancer microarray database and integrated data-mining platform. Neoplasia. 2004; 6(1): 1–6, doi: 10.1016/s1476-5586(04)80047-2, indexed in Pubmed: 15068665.
20. Dingerdissen HM, Bastian F, Vijay-Shanker K, et al. OncoMX: A Knowledgebase for Exploring Cancer Biomarkers in the Context of Related Cancer and Healthy Data. JCO Clin Cancer Inform. 2020; 4: 210–220, doi: 10.1200/CCI.19.00117, indexed in Pubmed: 32142370.
21. Chandrashekar DS, Karthikeyan SK, Korla PK, et al. UALCAN: An update to the integrated cancer data analysis platform. Neoplasia. 2022; 25: 18–27, doi: 10.1016/j.neo.2022.01.001, indexed in Pubmed: 35078134.
22. Xu S, Feng Y, Zhao S. Proteins with Evolutionarily Hypervariable Domains are Associated with Immune Response and Better Survival of Basal-like Breast Cancer Patients. Comput Struct Biotechnol J. 2019; 17: 430–440, doi: 10.1016/j.csbj.2019.03.008, indexed in Pubmed: 30996822.
23. Tang Z, Kang B, Li C, et al. GEPIA2: an enhanced web server for large-scale expression profiling and interactive analysis. Nucleic Acids Res. 2019; 47(W1): W556–W560, doi: 10.1093/nar/gkz430, indexed in Pubmed: 31114875.
24. Tang G, Cho M, Wang X. OncoDB: an interactive online database for analysis of gene expression and viral infection in cancer. Nucleic Acids Res. 2022; 50(D1): D1334–D1339, doi: 10.1093/nar/gkab970, indexed in Pubmed: 34718715.
25. Ru B, Sun J, Tong Y, et al. CR2Cancer: a database for chromatin regulators in human cancer. Nucleic Acids Res. 2018; 46(D1): D918–D924, doi: 10.1093/nar/gkx877, indexed in Pubmed: 29036683.
26. Li JH, Liu S, Zhou H, et al. starBase v2.0: decoding miRNA-ceRNA, miRNA-ncRNA and protein-RNA interaction networks from large-scale CLIP-Seq data. Nucleic Acids Res. 2014; 42(Database issue): D92–D97, doi: 10.1093/nar/gkt1248, indexed in Pubmed: 24297251.
27. Zengin T, Masud B, Önal-Süzek T. TCGAnalyzeR: a web application for integrative visualization of molecular and clinical data of cancer patients for cohort and associated gene discovery. Cancers (Basel). 2024; 16(2): 345–10.3390/cancers16020345, doi: 10.1101/2023.01.20.524925, indexed in Pubmed: 38254834.

28. Zhu Z, Zhou Q, Sun Y, et al. MethMarkerDB: a comprehensive cancer DNA methylation biomarker database. Nucleic Acids Res. 2024; 52(D1): D1380–D1392, doi: 10.1093/nar/gkad923, indexed in Pubmed: 37889076.
29. Díez-Villanueva A, Mallona I, Peinado MA. Wanderer, an interactive viewer to explore DNA methylation and gene expression data in human cancer. Epigenetics Chromatin. 2015; 8: 22, doi: 10.1186/s13072-015-0014-8, indexed in Pubmed: 26113876.
30. Jézéquel P, Gouraud W, Ben Azzouz F, et al. bc-GenExMiner 4.5: new mining module computes breast cancer differential gene expression analyses. Database (Oxford). 2021; 2021, doi: 10.1093/database/baab007, indexed in Pubmed: 33599248.
31. Ru B, Wong CN, Tong Y, et al. TISIDB: an integrated repository portal for tumor-immune system interactions. Bioinformatics. 2019; 35(20): 4200–4202, doi: 10.1093/bioinformatics/btz210, indexed in Pubmed: 30903160.
32. Yuan H, Yan M, Zhang G, et al. CancerSEA: a cancer single-cell state atlas. Nucleic Acids Res. 2019; 47(D1): D900–D908, doi: 10.1093/nar/gky939, indexed in Pubmed: 30329142.
33. Bartha Á, Győrffy B. TNMplot.com: A Web Tool for the Comparison of Gene Expression in Normal, Tumor and Metastatic Tissues. Int J Mol Sci. 2021; 22(5), doi: 10.3390/ijms22052622, indexed in Pubmed: 33807717.
34. Liu CH, Lai YL, Shen PC, et al. DriverDBv4: a multi-omics integration database for cancer driver gene research. Nucleic Acids Res. 2024; 52(D1): D1246–D1252, doi: 10.1093/nar/gkad1060, indexed in Pubmed: 37956338.
35. Győrffy B. Discovery and ranking of the most robust prognostic biomarkers in serous ovarian cancer. Geroscience. 2023; 45(3): 1889–1898, doi: 10.1007/s11357-023-00742-4, indexed in Pubmed: 36856946.
36. Xie Z, Bailey A, Kuleshov MV, et al. Gene Set Knowledge Discovery with Enrichr. Curr Protoc. 2021; 1(3): e90, doi: 10.1002/cpz1.90, indexed in Pubmed: 33780170.
37. Li T, Fan J, Wang B, et al. TIMER: A Web Server for Comprehensive Analysis of Tumor-Infiltrating Immune Cells. Cancer Res. 2017; 77(21): e108–e110, doi: 10.1158/0008-5472.CAN-17-0307, indexed in Pubmed: 29092952.

38. Chang Le, Xia J. MicroRNA Regulatory Network Analysis Using miRNet 2.0. Methods Mol Biol. 2023; 2594: 185–204, doi: 10.1007/978-1-0716-2815-7_14, indexed in Pubmed: 36264497.
39. Chou PH, Liao WC, Tsai KW, et al. TACCO, a Database Connecting Transcriptome Alterations, Pathway Alterations and Clinical Outcomes in Cancers. Sci Rep. 2019; 9(1): 3877, doi: 10.1038/s41598-019-40629-z, indexed in Pubmed: 30846808.
40. Li R, Qu H, Wang S, et al. CancerMIRNome: an interactive analysis and visualization database for miRNome profiles of human cancer. Nucleic Acids Res. 2022; 50(D1): D1139–D1146, doi: 10.1093/nar/gkab784, indexed in Pubmed: 34500460.
41. Li T, Fu J, Zeng Z, et al. TIMER2.0 for analysis of tumor-infiltrating immune cells. Nucleic Acids Res. 2020; 48(W1): W509–W514, doi: 10.1093/nar/gkaa407, indexed in Pubmed: 32442275.
42. Samaržija I, Tomljanović M, Novak Kujundžić R, et al. EZH2 Inhibition and Cisplatin as a Combination Anticancer Therapy: An Overview of Preclinical Studies. Cancers (Basel). 2022; 14(19), doi: 10.3390/cancers14194761, indexed in Pubmed: 36230683.
43. Mao Q, Wu P, Li H, et al. CRISPR/Cas9-mediated EZH2 knockout suppresses the proliferation and migration of triple-negative breast cancer cells. Oncol Lett. 2023; 26(2): 343, doi: 10.3892/ol.2023.13929, indexed in Pubmed: 37427349.
44. Verma A, Singh A, Singh MP, et al. EZH2-H3K27me3 mediated KRT14 upregulation promotes TNBC peritoneal metastasis. Nat Commun. 2022; 13(1): 7344, doi: 10.1038/s41467-022-35059-x, indexed in Pubmed: 36446780.
45. Wu SC, Zhang Yi. Cyclin-dependent kinase 1 (CDK1)-mediated phosphorylation of enhancer of zeste 2 (Ezh2) regulates its stability. J Biol Chem. 2011; 286(32): 28511–28519, doi: 10.1074/jbc.M111.240515, indexed in Pubmed: 21659531.
46. Chen S, Bohrer LR, Rai AN, et al. Cyclin-dependent kinases regulate epigenetic gene silencing through phosphorylation of EZH2. Nat Cell Biol. 2010; 12(11): 1108–1114, doi: 10.1038/ncb2116, indexed in Pubmed: 20935635.
47. Xia H, Zhang W, Li Y, et al. EZH2 silencing with RNA interference induces G2/M arrest in human lung cancer cells in vitro. Biomed Res Int. 2014; 2014: 348728, doi: 10.1155/2014/348728, indexed in Pubmed: 24745014.

Figure 1. Expression level of EZH2 by using: **A.** Cyclebase 3.0 shows the participation of EZH2 in S-Phase in cell cycle; **B.** Involvement of EZH2 in various cell development pathways using Cell Tracer; **C.** Expression of EZH2 in various cancer using Oncomine; **D.** Expression profile of EZH2 was determined by the UALCAN database for tumor versus normal samples; Red bars = Tumors, blue bars corresponding normal tissue

Figure 2. Expression of EZH2 in Breast Cancer. **A.–F.** mRNA expression was analyzed in normal breast tissue and primary tumors from the publicly available: **A.** UALCAN (Normal n = 114, Tumor n = 1097); **B.** TCGA Portal; **C.** GEPIA 2 (Normal n = 291, Tumor n = 1085); **D.** OncoDB; **E.** CR2cancer; **F.** ENCORI; **G.** Transcriptome analysis

Figure 3. EZH2 involvement in the methylation using: **A.** UALCAN (Normal n = 114, Tumor n = 1097); **B.–C.** CR2cancer (Normal *vs.* Tumor); **D.** OncoDB; **E.** MethMarkerDB

Figure 4 A.–E. EZH2 survival analysis. Kaplan-Meier survival curves were plotted for: **A.** Relapse-free survival (RFS); **B.** Overall survival (OS); **C.** Distant metastasis-free survival (DMFS). **D. PPS (E)** Multivariate analysis.

Figure 5. A.–E. mRNA expression of ESPL 1 in breast cancer aggressiveness and subtypes by using bc-GenExMiner v5.0; **F.** EZH2 gene expression with the breast cancer subtypes using TISIDB, UALCAN; **H.** By using bc-GenExMiner v5.0 database (Healthy *vs.* Tumor adjacent *vs.* BRCA subtypes); **I.** Expression analysis based on patient's age group using UALCAN

Figure 6. EZH2 expression in tumors from breast cancer patients with biological process and metastasis. **A.–E.** EZH2 expression in biological process using CancerSEA; **F.–H.** Metastasis in EZH2 expression normal, tumor, and metastasis in breast cancer patients using the Gene Chip and RNA — Chip using Tumor Node Metastasis Plot (TNM plot) and DriverDB database

Figure 7. A.–D. Correlation between the EZH2 and E2Fs using ENCORI database; **E.–H.** EZH2 and E2Fs family expression using TIMER database; **I.–L.** OcoBD database; **M.–P.** GEPIA2.0 database

Figure 8. ceRNA network analysis with EZH2 in tumor tissues from breast cancer patients determined by using TACCO, CancerMIRNome, ENCORI, UALCAN, and database **(A-C** respectively). **A.** Transcriptome analysis using TACCO; **B.** correlation between the EZH2 and let-7b-5p using CancerMIRNome; **C.** Boxplot of correlation between let-7b-5p and EZH2; **D.** hsa-let-7b-5p expression in Tumor *vs.* Normal using CancerMIRNome; **E.** Boxplot of let-7b-5p expression in breast cancer (n = 149) *vs.* normal (n = 78) using UALCAN; **F.–H.** Using

ENCORI, GEPIA and TIMER databases showing box-plot of correlation between TMPO-AS1 and EZH2; **I.–J.** Boxplot TMPO-AS1 gene expression in normal vs tumor using UALCAN and OncoDB database

Table 1. Correlation of EZH2 *vs.* miRNAs

S.no	miRNA	Correlation
1	hsa-let-7b-5p	–0.289
2	hsa-let-7e-5p	0.031
3	hsa-mir-26a-5p	–0.091
4	hsa-mir-27a-3p	0.174
5	hsa-mir-101-3p	–0.16
6	hsa-mir-214-3p	–0.072
7	hsa-mir-217	–0.013
8	hsa-mir-200b-3p	0.164
9	hsa-mir-137	0.100
10	hsa-mir-150-5p	0.182
11	hsa-mir-429	0.215
12	hsa-mir-19a-3p	0.461
13	hsa-mir-27b-3p	0.087
14	hsa-mir-29a-3p	0.009
15	hsa-mir-29b-3p	0.055
16	hsa-mir-29c-3p	–0.262
17	hsa-mir-34a-5p	0.042
18	hsa-mir-1-3p	–0.159
19	hsa-mir-155-5p	0.334
20	hsa-mir-16-5p	0.267
21	hsa-mir-7-5p	Positive
22	hsa-miR-101-3p	0.305
23	hsa-mir-30d-5p	0.035
24	hsa-mir-27a-3p	0.174

Table 2. Correlation of EZH2 *vs.* lncRNAs

Index	Name	Correlation value with EZH2	p-value
1	TMPO-AS1	0.587	4.16e–103
2	PRC1-AS1	0.335	2.19e–30
3	LINC01775	0.350	4.07e–33
4	DEPDC1-AS1	0.480	1.12e–64

Figure 1

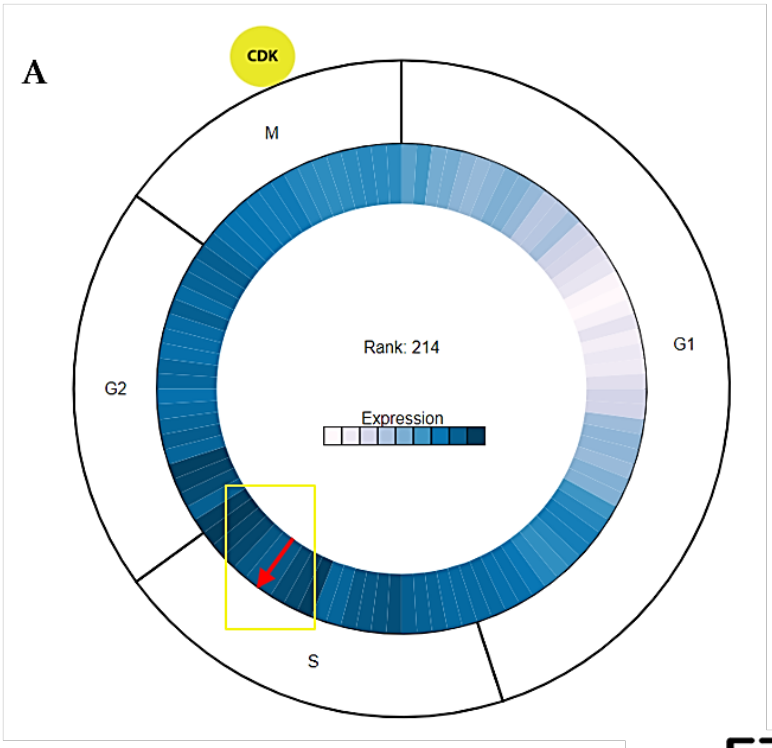
A
CDK
M
G1
G2
S
Rank: 214
Expression

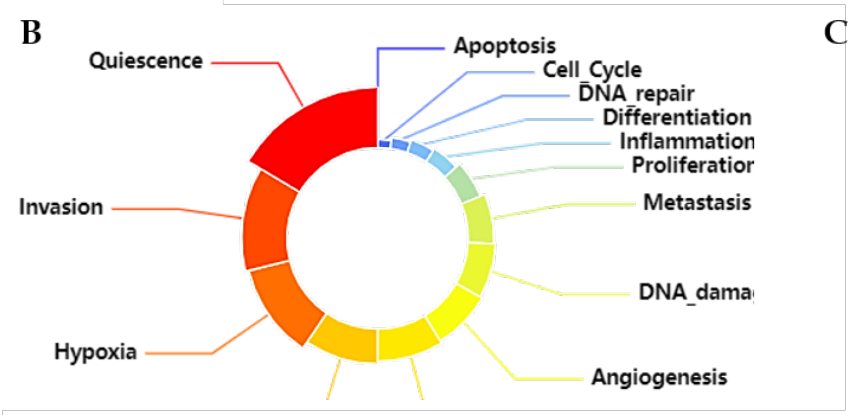
B
Quiescence
Apoptosis
Cell_Cycle
DNA_repair
Differentiation
Inflammation
Proliferatior
Metastasis
DNA_dama
Angiogenesis
Hypoxia
Invasion

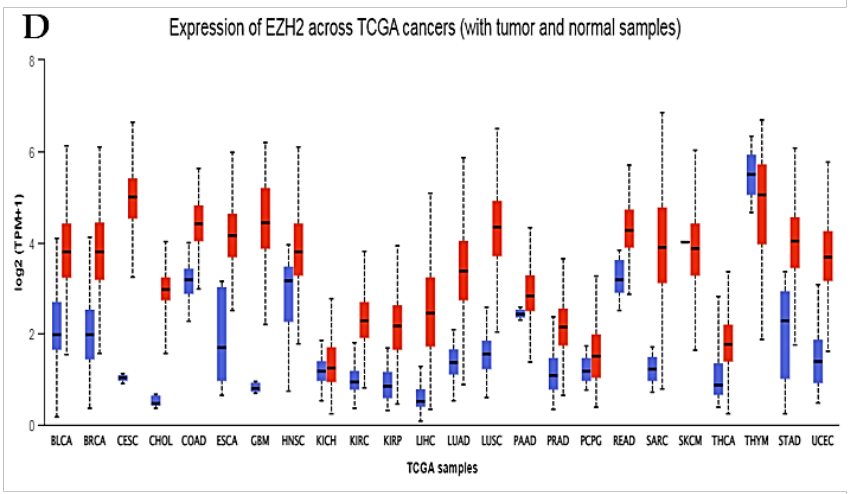
D
Expression of EZH2 across TCGA cancers (with tumor and normal samples)
log2 (TPM+1)
BLCA BRCA CESC CHOL COAD ESCA GBM HNSC KICH KIRC KIRP LIHC LUAD LUSC PAAD PRAD PCPG READ SARC SKCM THCA THYM STAD UCEC
TCGA samples

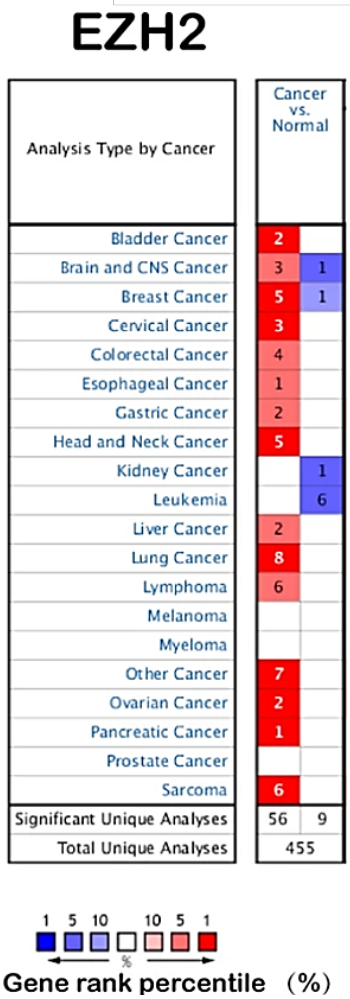
C
EZH2
Analysis Type by Cancer
Cancer vs. Normal
Bladder Cancer 2
Brain and CNS Cancer 3 1
Breast Cancer 5 1
Cervical Cancer 3
Colorectal Cancer 4
Esophageal Cancer 1
Gastric Cancer 2
Head and Neck Cancer 5
Kidney Cancer 1
Leukemia 6
Liver Cancer 2
Lung Cancer 8
Lymphoma 6
Melanoma
Myeloma
Other Cancer 7
Ovarian Cancer 2
Pancreatic Cancer 1
Prostate Cancer
Sarcoma 6
Significant Unique Analyses 56 9
Total Unique Analyses 455
1 5 10 10 5 1
%
Gene rank percentile (%)

Figure 2

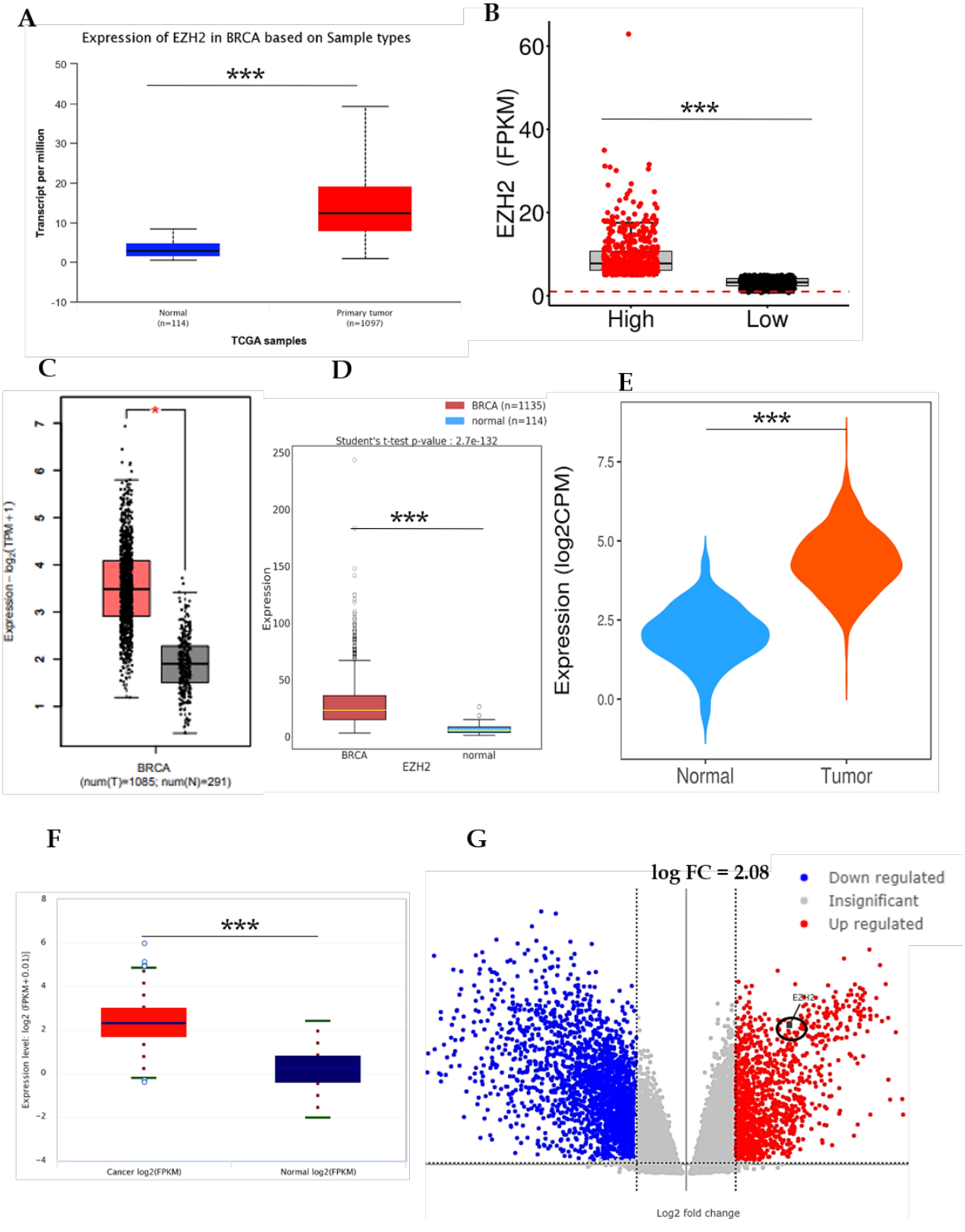
A
Expression of EZH2 in BRCA based on Sample types
***
Transcript per million
Normal (n=114)
Primary tumor (n=1097)
TCGA samples
B
***
EZH2 (FPKM)
High
Low
C
Expression – log2(TPM+1)
BRCA (num(T)=1085; num(N)=291)
D
BRCA (n=1135)
normal (n=114)
Student's t-test p-value : 2.7e-132
***
Expression
BRCA
normal
EZH2
E
***
Expression (log2CPM)
Normal
Tumor
F
***
Expression level: log2 (FPKM+0.01)]
Cancer log2(FPKM)
Normal log2(FPKM)
G
log FC = 2.08
Down regulated
Insignificant
Up regulated
EZH2
Log2 fold change

Figure 3

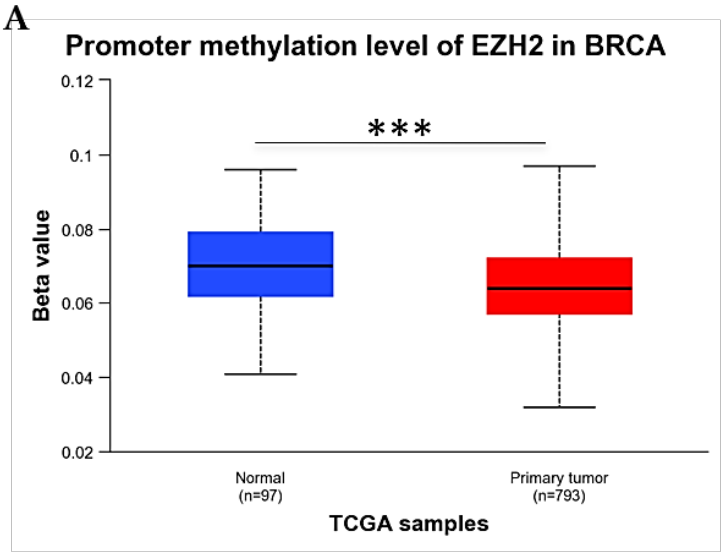
A
Promoter methylation level of EZH2 in BRCA
***
Beta value
0.12
0.1
0.08
0.06
0.04
0.02
Normal
(n=97)
Primary tumor
(n=793)
TCGA samples

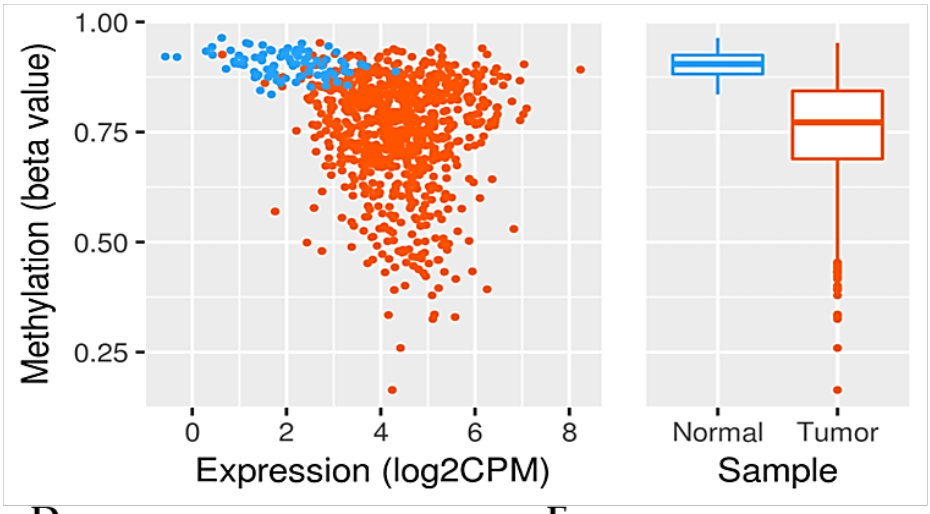
B
C
Methylation (beta value)
1.00
0.75
0.50
0.25
0
2
4
6
8
Expression (log2CPM)
Normal
Tumor
Sample

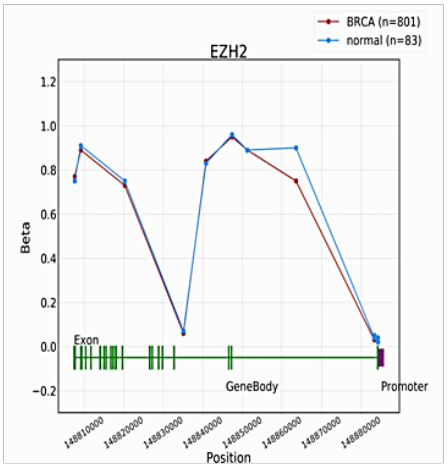
D
BRCA (n=801)
normal (n=83)
EZH2
Beta
Exon
GeneBody
Promoter
Position

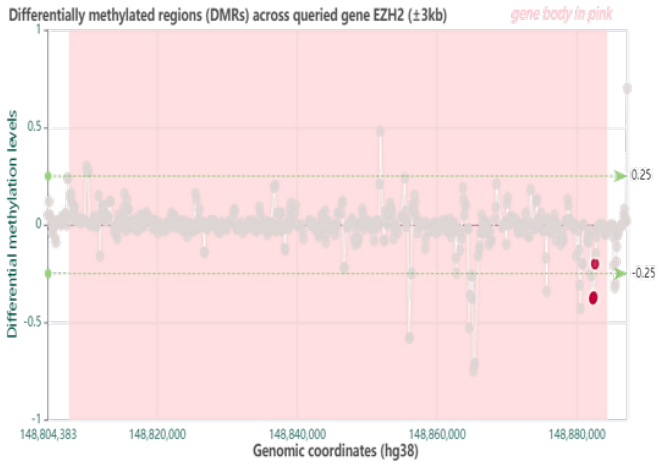
E
Differentially methylated regions (DMRs) across queried gene EZH2 (±3kb)
gene body in pink
Differential methylation levels
0.25
-0.25
148,804,383
148,820,000
148,840,000
148,860,000
148,880,000
Genomic coordinates (hg38)

Figure 5

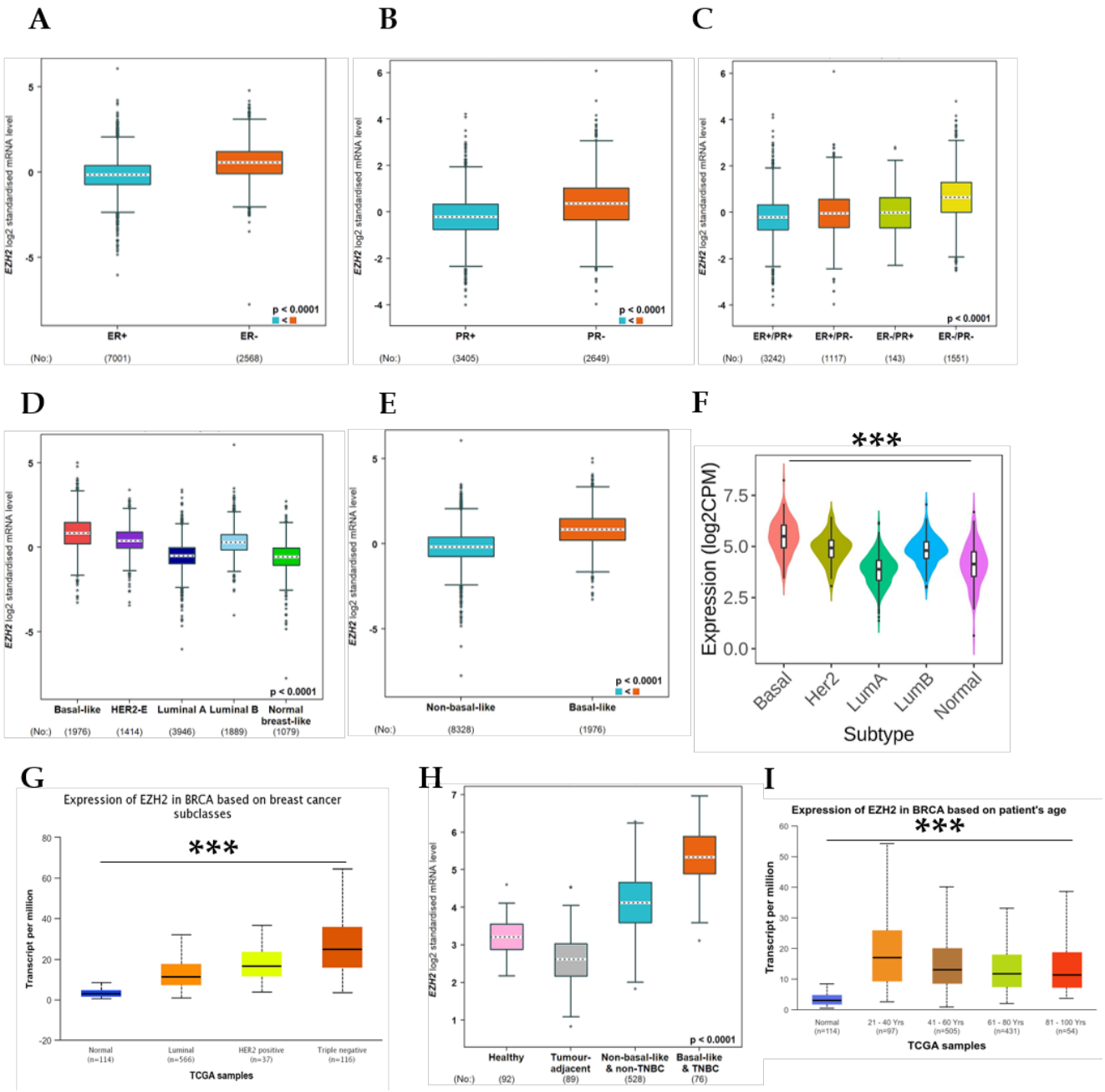
A
B
C
EZH2 log2 standardised mRNA level
p < 0.0001
ER+
ER-
(No:)
(7001)
(2568)
PR+
PR-
(3405)
(2649)
ER+/PR+
ER+/PR-
ER-/PR+
ER-/PR-
(3242)
(1117)
(143)
(1551)
D
E
F
Basal-like
HER2-E
Luminal A
Luminal B
Normal breast-like
(1976)
(1414)
(3946)
(1889)
(1079)
Non-basal-like
Basal-like
(8328)
(1976)
***
Expression (log2CPM)
Basal
Her2
LumA
LumB
Normal
Subtype
G
H
I
Expression of EZH2 in BRCA based on breast cancer subclasses
Transcript per million
Normal (n=114)
Luminal (n=566)
HER2 positive (n=37)
Triple negative (n=116)
TCGA samples
Healthy
Tumour-adjacent
Non-basal-like & non-TNBC
Basal-like & TNBC
(92)
(89)
(528)
(76)
Expression of EZH2 in BRCA based on patient's age
Normal (n=114)
21 - 40 Yrs (n=97)
41 - 60 Yrs (n=505)
61 - 80 Yrs (n=431)
81 - 100 Yrs (n=54)

Figure 6

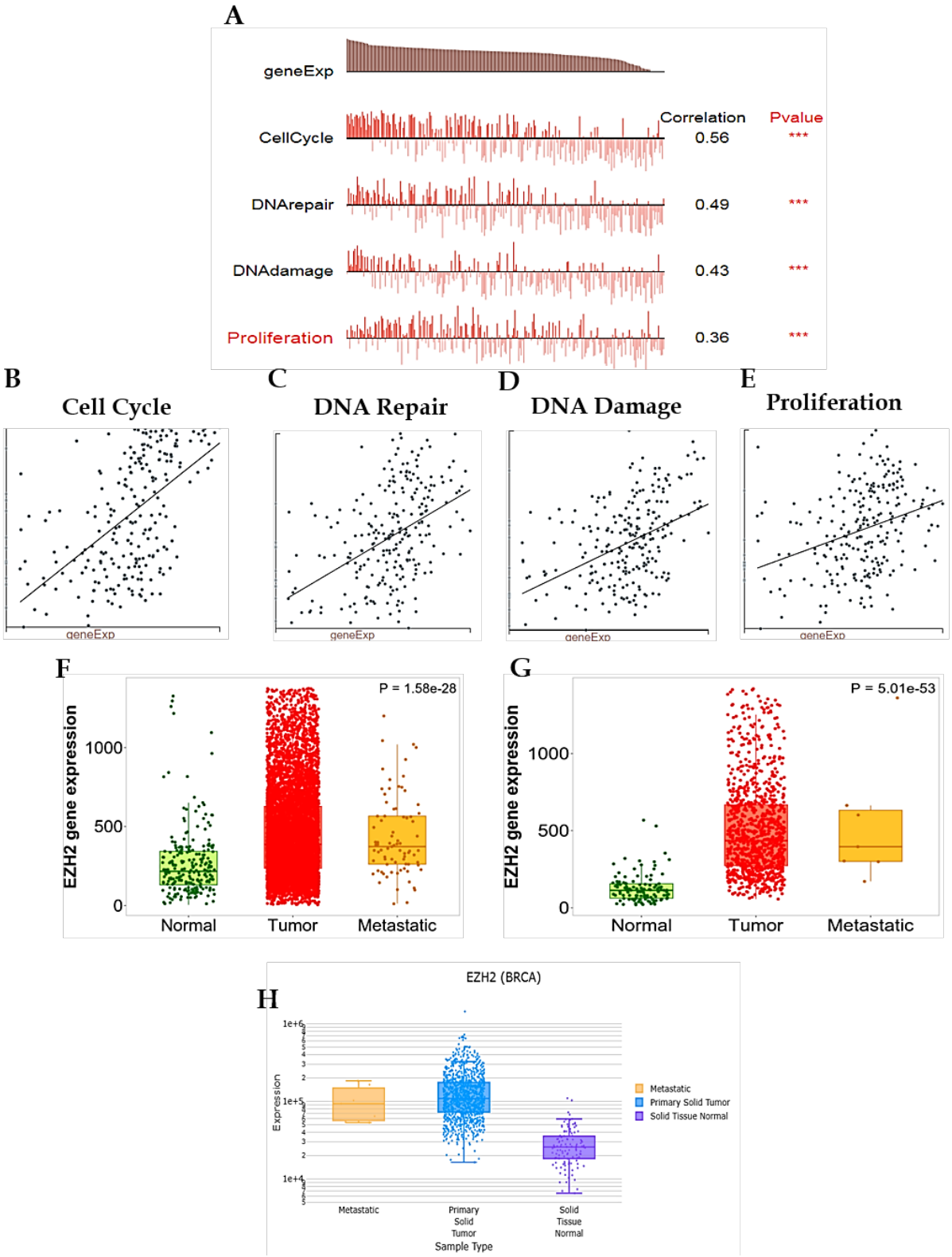
A
geneExp
Correlation
Pvalue
CellCycle
0.56
***
DNArepair
0.49
***
DNAdamage
0.43
***
Proliferation
0.36
***
B
Cell Cycle
C
DNA Repair
D
DNA Damage
E
Proliferation
geneExp
F
P = 1.58e-28
EZH2 gene expression
1000
500
0
Normal
Tumor
Metastatic
G
P = 5.01e-53
EZH2 gene expression
1000
500
0
Normal
Tumor
Metastatic
H
EZH2 (BRCA)
Expression
1e+6
1e+5
1e+4
Metastatic
Primary Solid Tumor
Solid Tissue Normal
Metastatic
Primary Solid Tumor
Solid Tissue Normal
Sample Type

Figure 7

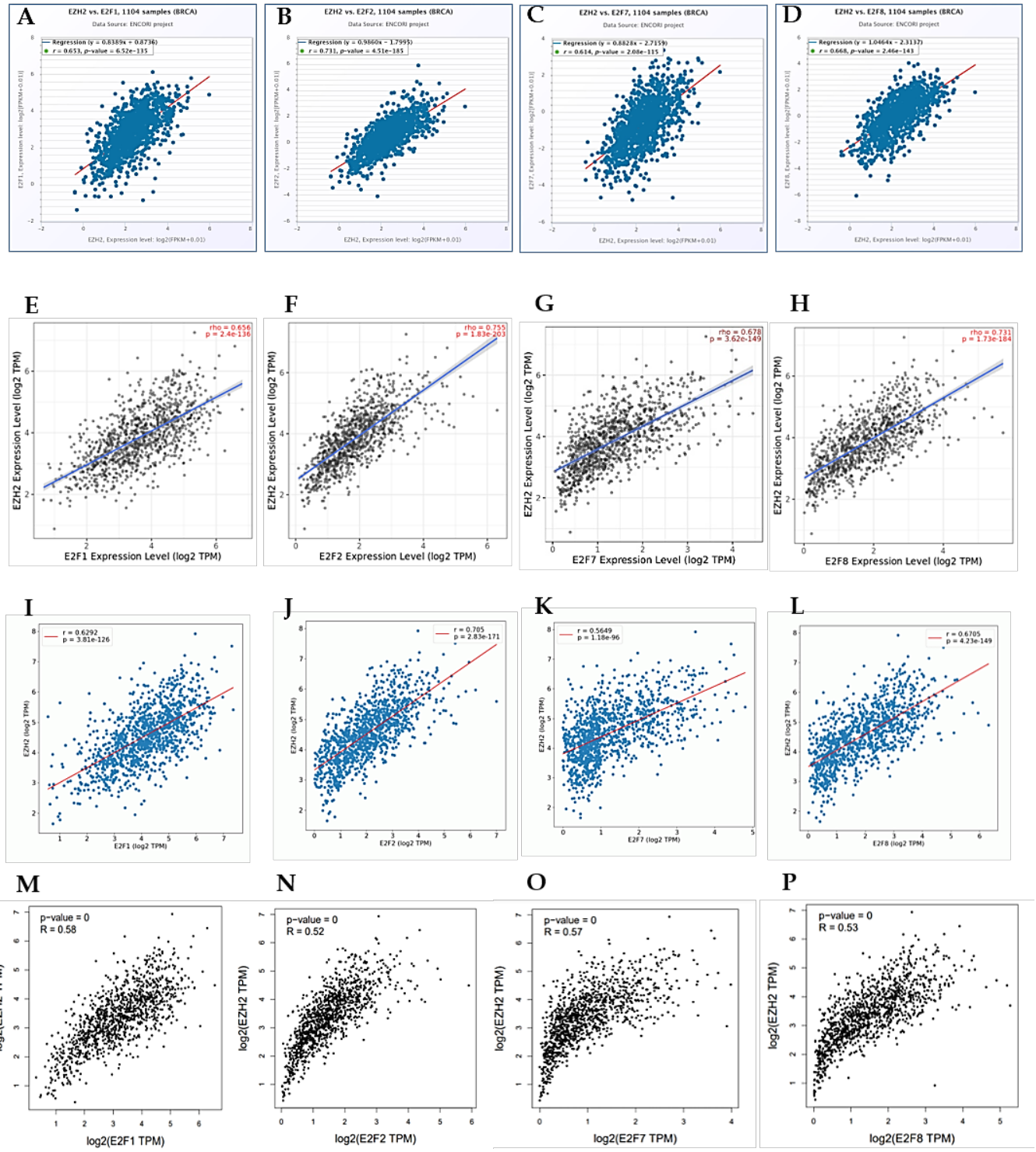
A
EZH2 vs. E2F1, 1104 samples (BRCA)
Data Source: ENCORI project
Regression (y = 0.8389x + 0.8736)
r = 0.653, p-value = 6.52e-135
EZH2, Expression level: log2(FPKM+0.01)
B
EZH2 vs. E2F2, 1104 samples (BRCA)
Data Source: ENCORI project
Regression (y = 0.9860x - 1.7995)
r = 0.731, p-value = 4.51e-185
EZH2, Expression level: log2(FPKM+0.01)
C
EZH2 vs. E2F7, 1104 samples (BRCA)
Data Source: ENCORI project
Regression (y = 0.8828x - 2.7159)
r = 0.614, p-value = 2.08e-115
EZH2, Expression level: log2(FPKM+0.01)
D
EZH2 vs. E2F8, 1104 samples (BRCA)
Data Source: ENCORI project
Regression (y = 1.0464x - 2.3137)
r = 0.668, p-value = 2.46e-143
EZH2, Expression level: log2(FPKM+0.01)
E
rho = 0.656
p = 2.4e-136
EZH2 Expression Level (log2 TPM)
E2F1 Expression Level (log2 TPM)
F
rho = 0.755
p = 1.83e-203
EZH2 Expression Level (log2 TPM)
E2F2 Expression Level (log2 TPM)
G
rho = 0.678
p = 3.62e-149
EZH2 Expression Level (log2 TPM)
E2F7 Expression Level (log2 TPM)
H
rho = 0.731
p = 1.73e-184
EZH2 Expression Level (log2 TPM)
E2F8 Expression Level (log2 TPM)
I
r = 0.6292
p = 3.81e-126
EZH2 (log2 TPM)
E2F1 (log2 TPM)
J
r = 0.705
p = 2.83e-171
EZH2 (log2 TPM)
E2F2 (log2 TPM)
K
r = 0.5649
p = 1.18e-96
EZH2 (log2 TPM)
E2F7 (log2 TPM)
L
r = 0.6705
p = 4.23e-149
EZH2 (log2 TPM)
E2F8 (log2 TPM)
M
p-value = 0
R = 0.58
log2(EZH2 TPM)
log2(E2F1 TPM)
N
p-value = 0
R = 0.52
log2(EZH2 TPM)
log2(E2F2 TPM)
O
p-value = 0
R = 0.57
log2(EZH2 TPM)
log2(E2F7 TPM)
P
p-value = 0
R = 0.53
log2(EZH2 TPM)
log2(E2F8 TPM)

Figure 8

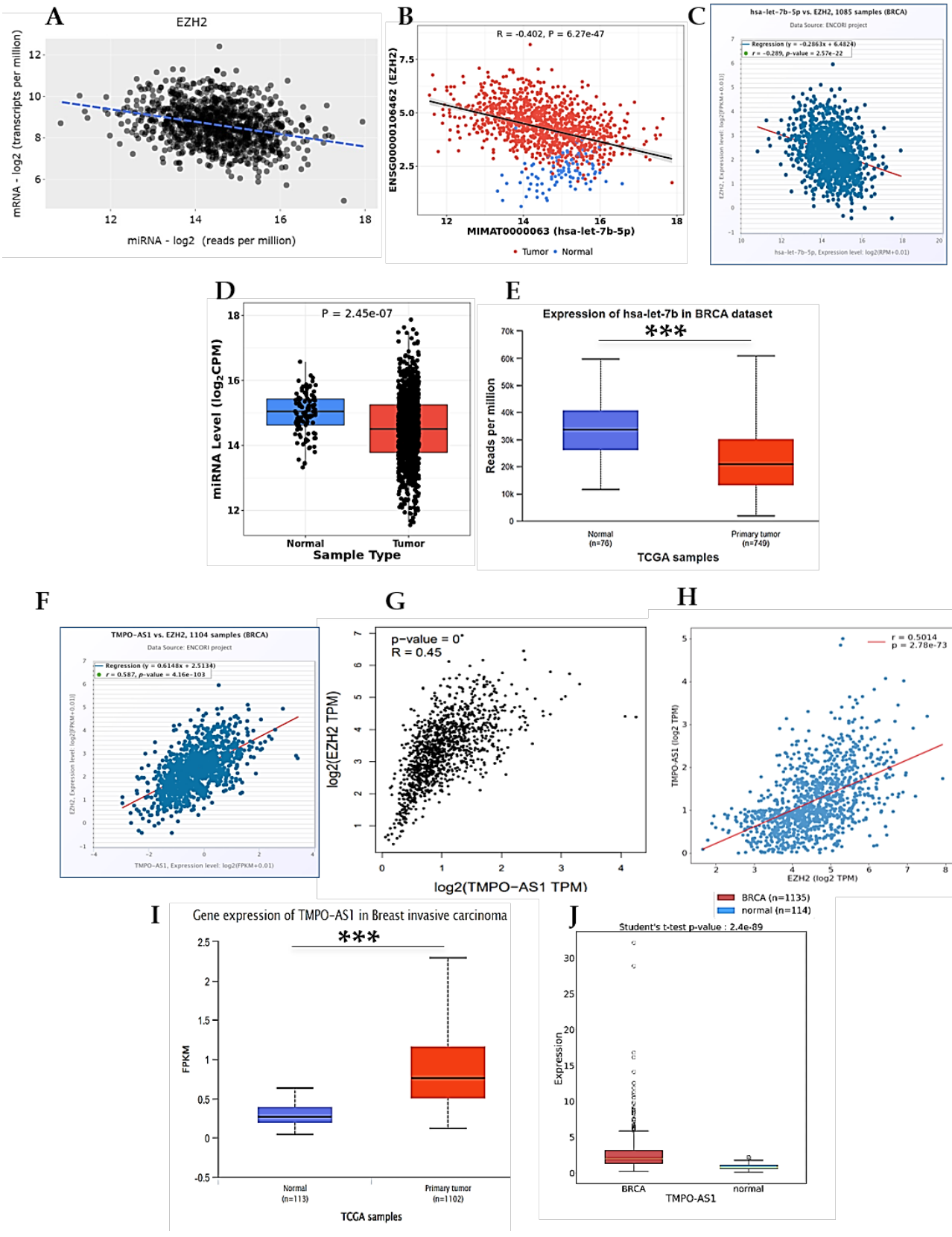
A
EZH2
mRNA - log2 (transcripts per million)
miRNA - log2 (reads per million)
B
R = -0.402, P = 6.27e-47
ENSG00000106462 (EZH2)
MIMAT0000063 (hsa-let-7b-5p)
Tumor
Normal
C
hsa-let-7b-5p vs. EZH2, 1085 samples (BRCA)
Data Source: ENCORI project
D
P = 2.45e-07
miRNA Level (log2CPM)
Normal
Tumor
Sample Type
E
Expression of hsa-let-7b in BRCA dataset
***
Reads per million
Normal (n=76)
Primary tumor (n=749)
TCGA samples
F
TMPO-AS1 vs. EZH2, 1104 samples (BRCA)
Data Source: ENCORI project
G
p-value = 0*
R = 0.45
log2(EZH2 TPM)
log2(TMPO-AS1 TPM)
H
r = 0.5014
p = 2.78e-73
TMPO-AS1 (log2 TPM)
EZH2 (log2 TPM)
I
Gene expression of TMPO-AS1 in Breast invasive carcinoma
***
FPKM
Normal (n=113)
Primary tumor (n=1102)
TCGA samples
J
BRCA (n=1135)
normal (n=114)
Student's t-test p-value : 2.4e-89
Expression
BRCA
normal
TMPO-AS1

Supplementary File

Figure S1. A-C. TCGA Wanderer was used to compare the methylation status of EZH2 in (n= 30) normal sample vs. (n = 30) BRCA tumor

Figure S2. Correlation by using ENCORI database. **A.–B.** Molecular mechanism of regulatory network associated with ESR1 and PGR genes; **C.** Boxplot of correlation between E2F3 and ESPL1; **D** Boxplot of E2F4 and EZH2; **E.** Boxplot of E2F5 and EZH2; F. Boxplot of E2F6 and EZH2

Figure S3. Molecular mechanism of regulatory network associated with ESR1, PGR genes with the E2F by using ENCORI. Correlation between: **A.** E2F1 *vs.* ESR1; **B.** E2F2 *vs.* ESR1; **C.** E2F7 *vs.* ESR1; **D.** E2F8 *vs.* ESR1; **E.** E2F1 *vs.* PGR; **F.** E2F2 *vs.* PGR; **G.** E2F7 *vs.* PGR; **H.** E2F8 *vs.* PGR was evaluated

Figure S4. A. miRNAs associated with the ESPL1 using miRNet database; **B.–D.** let-7b-5p survival analysis using CancerMIRNome, KM Plotter and ENCORI respectively; **E.–F.** Correlation of let-7b-5p with E2F7/E2F8 using ENCORI database; **E.** TMPO-AS1 lncRNA network was created with ESPL1/let-7b-5p using miRNet database

Figure S5. ENCORI database showing: **A.** Correlation between TMPO-AS1 and E2F2; **B.** Correlation between TMPO-AS1 and let-7b-5p; **C.** Correlation between TMPO-AS1 and ESR1; **D.** Correlation between TMPO-AS1 and PGR; **E.** MiRNet database showing the network of EZH2, hsa-let-7b-5p and TMPO-AS1

Table S1. Role of EZH2

Biological Process	GO:0000082 G1/S transition of mitotic cell cycle GO:0000302 response to reactive oxygen species GO:0001837 epithelial to mesenchymal transition GO:0001889 liver development GO:0003012 muscle system process GO:0003299 muscle hypertrophy in response to stress GO:0003300 cardiac muscle hypertrophy GO:0006304 DNA modification

	GO:0006305 DNA alkylation GO:0006306 DNA methylation GO:0006354 DNA-templated transcription, elongation GO:0006368 transcription elongation from RNA polymerase II promoter GO:0006479 protein methylation GO:0006979 response to oxidative stress GO:0007346 regulation of mitotic cell cycle GO:0007623 circadian rhythm GO:0008213 protein alkylation GO:0008544 epidermis development GO:0009913 epidermal cell differentiation GO:0010035 response to inorganic substance GO:0010717 regulation of epithelial to mesenchymal transition GO:0010718 positive regulation of epithelial to mesenchymal transition GO:0010720 positive regulation of cell development GO:0010948 negative regulation of cell cycle process GO:0010975 regulation of neuron projection development GO:0010976 positive regulation of neuron projection development GO:0014013 regulation of gliogenesis GO:0014834 skeletal muscle satellite cell maintenance involved in skeletal muscle regeneration GO:0014887 cardiac muscle adaptation GO:0014888 striated muscle adaptation GO:0014896 muscle hypertrophy GO:0014897 striated muscle hypertrophy GO:0014898 cardiac muscle hypertrophy in response to stress GO:0016358 dendrite development GO:0016570 histone modification GO:0016571 histone methylation GO:0018022 peptidyl-lysine methylation

	GO:0018205 peptidyl-lysine modification GO:0021537 telencephalon development GO:0021543 pallium development GO:0021549 cerebellum development GO:0021695 cerebellar cortex development GO:0021761 limbic system development GO:0021766 hippocampus development GO:0022037 metencephalon development GO:0030522 intracellular receptor signaling pathway GO:0030856 regulation of epithelial cell differentiation GO:0030857 negative regulation of epithelial cell differentiation GO:0030900 forebrain development GO:0030902 hindbrain development GO:0031099 regeneration GO:0031100 animal organ regeneration GO:0031346 positive regulation of cell projection organization GO:0032259 methylation GO:0032355 response to estradiol GO:0032784 regulation of DNA-templated transcription, elongation GO:0032785 negative regulation of DNA-templated transcription, elongation GO:0033674 positive regulation of kinase activity GO:0034243 regulation of transcription elongation from RNA polymerase II promoter GO:0034244 negative regulation of transcription elongation from RNA polymerase II promoter GO:0034502 protein localization to chromosome GO:0034599 cellular response to oxidative stress GO:0034614 cellular response to reactive oxygen species GO:0034968 histone lysine methylation

	GO:0035983 response to trichostatin A GO:0035984 cellular response to trichostatin A GO:0036333 hepatocyte homeostasis GO:0040029 regulation of gene expression, epigenetic GO:0042063 gliogenesis GO:0042246 tissue regeneration GO:0042542 response to hydrogen peroxide GO:0042692 muscle cell differentiation GO:0042752 regulation of circadian rhythm GO:0043403 skeletal muscle tissue regeneration GO:0043405 regulation of MAP kinase activity GO:0043406 positive regulation of MAP kinase activity GO:0043410 positive regulation of MAPK cascade GO:0043414 macromolecule methylation GO:0043433 negative regulation of sequence-specific DNA binding transcription factor activity GO:0043500 muscle adaptation GO:0044728 DNA methylation or demethylation GO:0044770 cell cycle phase transition GO:0044772 mitotic cell cycle phase transition GO:0044843 cell cycle G1/S phase transition GO:0045604 regulation of epidermal cell differentiation GO:0045605 negative regulation of epidermal cell differentiation GO:0045666 positive regulation of neuron differentiation GO:0045682 regulation of epidermis development GO:0045683 negative regulation of epidermis development GO:0045786 negative regulation of cell cycle GO:0045814 negative regulation of gene expression, epigenetic GO:0045860 positive regulation of protein kinase activity GO:0045930 negative regulation of mitotic cell cycle

	GO:0046677 response to antibiotic GO:0048384 retinoic acid receptor signaling pathway GO:0048385 regulation of retinoic acid receptor signaling pathway GO:0048387 negative regulation of retinoic acid receptor signaling pathway GO:0048511 rhythmic process GO:0048732 gland development GO:0048762 mesenchymal cell differentiation GO:0048872 homeostasis of number of cells GO:0050769 positive regulation of neurogenesis GO:0050773 regulation of dendrite development GO:0051090 regulation of sequence-specific DNA binding transcription factor activity GO:0051146 striated muscle cell differentiation GO:0051147 regulation of muscle cell differentiation GO:0051148 negative regulation of muscle cell differentiation GO:0051153 regulation of striated muscle cell differentiation GO:0051154 negative regulation of striated muscle cell differentiation GO:0051962 positive regulation of nervous system development GO:0060485 mesenchyme development GO:0061008 hepaticobiliary system development GO:0070301 cellular response to hydrogen peroxide GO:0070314 G1 to G0 transition GO:0070734 histone H3-K27 methylation GO:0071168 protein localization to chromatin GO:0071236 cellular response to antibiotic GO:0071407 cellular response to organic cyclic compound GO:0071417 cellular response to organonitrogen compound GO:0071900 regulation of protein serine/threonine kinase activity GO:0071902 positive regulation of protein serine/threonine kinase activity

	GO:0097421 liver regeneration GO:0098532 histone H3-K27 trimethylation GO:0098727 maintenance of cell number GO:1900006 positive regulation of dendrite development GO:1901987 regulation of cell cycle phase transition GO:1901988 negative regulation of cell cycle phase transition GO:1901990 regulation of mitotic cell cycle phase transition GO:1901991 negative regulation of mitotic cell cycle phase transition GO:1902806 regulation of cell cycle G1/S phase transition GO:1902807 negative regulation of cell cycle G1/S phase transition GO:1904772 response to tetrachloromethane GO:2000045 regulation of G1/S transition of mitotic cell cycle GO:2000134 negative regulation of G1/S transition of mitotic cell cycle
Molecular Function	GO:0000979 RNA polymerase II core promoter sequence-specific DNA binding GO:0001046 core promoter sequence-specific DNA binding GO:0001047 core promoter binding GO:0003682 chromatin binding GO:0008168 methyltransferase activity GO:0008170 N-methyltransferase activity GO:0008276 protein methyltransferase activity GO:0008757 S-adenosylmethionine-dependent methyltransferase activity GO:0016278 lysine N-methyltransferase activity GO:0016279 protein-lysine N-methyltransferase activity GO:0016741 transferase activity, transferring one-carbon groups GO:0018024 histone-lysine N-methyltransferase activity GO:0031490 chromatin DNA binding GO:0042054 histone methyltransferase activity GO:0043021 ribonucleoprotein complex binding GO:0043566 structure-specific DNA binding

	GO:0046976 histone methyltransferase activity (H3-K27 specific) GO:0070878 primary miRNA binding GO:1990841 promoter-specific chromatin binding
Cellular Component	GO:0000785 chromatin GO:0000790 nuclear chromatin GO:0031519 PcG protein complex GO:0034708 methyltransferase complex GO:0035097 histone methyltransferase complex GO:0035098 ESC/E(Z) complex GO:0044454 nuclear chromosome part GO:0045120 pronucleus
KEGG	hsa00310 Lysine degradation
Reactome	R-HSA-5619507: Activation of HOX genes during differentiation R-HSA-5617472: Activation of anterior HOX genes in hindbrain development during early embryogenesis R-HSA-2559583: Cellular Senescence R-HSA-2262752: Cellular responses to stress R-HSA-3247509: Chromatin modifying enzymes R-HSA-4839726: Chromatin organization R-HSA-1266738: Developmental Biology R-HSA-212165: Epigenetic regulation of gene expression R-HSA-74160: Gene Expression R-HSA-2559580: Oxidative Stress Induced Senescence R-HSA-3214841: PKMTs methylate histone lysines R-HSA-212300: PRC2 methylates histones and DNA

Table S2. EZH2 Pan-Cancer analysis

UniProtKB/SwissProt AC	Gene Symbol	Log2 F.C.	P-value	Adj. P-value	Significant	Expression Trend	TCGA Study
Q15910	EZH2	0.45	0.000252	0.00067	Yes	Up	Thyroid cancer
		1.4	1.53e-21	1.24e-19	Yes	Up	Stomach cancer
		2.41	1.81e-62	7.41e-60	Yes	Up	Liver cancer
		2.6	7.37e-74	2.38e-71	Yes	Up	Uterine cancer
		1.73	1.25e-15	6.71e-14	Yes	Up	Bladder cancer
		0.69	1.77e-7	8.94e-7	Yes	Up	Head_and_neck cancer
		2.96	4.91e-213	2.16e-210	Yes	Up	Lung cancer
		1.44	1.98e-12	2.95e-10	Yes	Up	Esophageal cancer
		1.27	1.96e-65	1.83e-63	Yes	Up	Colorectal cancer
		1.4	6.38e-37	1.21e-34	Yes	Up	Prostate cancer
		1.79	4.16e-131	1.19e-128	Yes	Up	Kidney cancer
		2.32	**1.33e-139**	**2.88e-137**	**Yes**	**Up**	**Breast cancer**

Table S3. Pan-Cancer methylation analysis

Cancer	Full Name	R	P	# N	# T	Delta beta (T *vs.* N)	P value (T *vs.* N)
BRCA	Breast invasive carcinoma	–0.277	1.27e–16	83	785	–0.133	2.29e–110
UCEC	Uterine Corpus Endometrial Carcinoma	–0.247	7.57e–08	34	431	–0.123	2.17e–10
BLCA	Bladder urothelial	–0.293	9.47e–10	17	408	–0.088	0.000374

	carcinoma						
KIRC	Kidney renal clear cell	–0.248	3.59e–06	24	319	–0.068	3.25e–33

S.NO.	Gene	Index	Patient Number	Hazard Ratio	CI	Log(P)	Low Expression Cohort (Months)	High Expression Cohort (Months)
1	EZH2	RFS	4929	1.5	1.36-1.67	6.2e-15	72	35
		OS	1879	1.31	1.08-1.58	0.0063	118.82	75.37
		DMFS	2765	1.45	1.24-1.7	3.9e-06	114.02	56.4
		PPS	458	1.47	1.16-1.86	0.0012	42.48	24.6

Table S4. Survival analysis

Table S5. Correlation with cell cycle checkpoints

S.No.	Gene	Cyclin D (CCND1)		Cyclin E (CCNE1)	Cyclin A (CCNA1)	Cyclin B (CCNB1)
1	EZH2	–0.22		0.67	0.15	0.67
		CDKs				
		4	6	2	2	1
		0.29	0.19	0.57	0.57	0.69

Table S6. Associated transcription factors

Index	Name	P-value	Adjusted p-value	Odds Ratio	Combined score
1	E2F1	0.001714	0.03044	40.05	255.08
2	PML	0.003382	0.03044	28.14	160.12
3	POLE	0.008966	0.04513	130.54	615.43
4	MYC	0.01018	0.04513	8.55	39.23

Index	Name	P-value	Adjusted p-value	Odds Ratio	Combined score
5	E2F2	0.01490	0.04513	76.48	321.69

Table S7. lncRNA analysis

Index	Name	p-value	Adjusted p-value	Odds ratio	Combined score
1	TMPO-AS1	1.31E-17	1.05E-15	865.13	33631.66
2	PRC1-AS1	7.48E-15	1.20E-13	499.21	16237.8
3	RRM1-AS1	7.48E-15	1.20E-13	499.21	16237.8
4	H2AZ1-DT	7.48E-15	1.20E-13	499.21	16237.8
5	LINC01775	7.48E-15	1.20E-13	499.21	16237.8
6	SGO1-AS1	2.77E-12	2.46E-11	317.49	8448.82
7	DEPDC1-AS1	2.77E-12	2.46E-11	317.49	8448.82
8	HMMR-AS1	2.77E-12	2.46E-11	317.49	8448.82
9	UBL7-AS1	2.77E-12	2.46E-11	317.49	8448.82
10	APOBEC3B-AS1	1.21E-07	7.43E-07	138.15	2200.74

Table S8. Differential expression analysis of lncRNAs

Index	Name	Downregulated/Upregulated in BRCA	p-value
1	TMPO-AS1	Upregulated	9.07e–104
2	PRC1-AS1	Upregulated	6.40e–03
3	RRM1-AS1	Downregulated	6.62e–08
4	H2AZ1-DT	Downregulated	7.04e–02
5	LINC01775	Upregulated	1.37e–65
6	SGO1-AS1	Downregulated	9.94e–01
7	DEPDC1-AS1	Upregulated	5.20e–43
8	HMMR-AS1	Downregulated	2.38e–16
9	UBL7-AS1	Downregulated	8.52e–06
10	APOBEC3B-AS1	Downregulated	4.70e–01

Table S9. EZH2 expression with positive correlator drugs

Gene symbol	Drug name	Correlation	FDR
GDSC			
EZH2	Trametinib	0.38	0.00e+0
	17-AAG	0.37	0.00e+0
	RDEA119	0.33	0.00e+0
	Docetaxel	0.31	0.00e+0
	selumetinib	0.30	0.00e+0
	PD-0325901	0.28	0.00e+0
	Lapatinib	0.24	1.94e–5
	Erlotinib	0.24	1.43e–4
	Afatinib	0.23	6.10e–12
	Dasatinib	0.22	1.57e–4
CTRP			
EZH2	VAF-347	0.19	8.61e–4
	Myriocin	0.18	0.67
	BRD-K99006945	0.14	0.04
	Dasatinib	0.14	1.06e–3
	Vandetanib	0.13	3.74e–3
	Erlotinib	0.12	3.05e–3
	Ifosfamide	0.12	0.48
	Selumetinib	0.12	6.90e–3
	ML334 diastereomer	0.12	0.06
	BEC	0.12	1.00

Table S10. EZH2 expression with negative correlator drugs

Gene symbol	Drug name	Correlation	FDR
GDSC			
EZH2	NPK76-II-72-1	–0.41	1.97e–36
	Navitoclax	–0.35	3.23e–25
	BX-912	–0.35	5.35e–26
	GSK1070916	–0.34	7.52e–25
	WZ3105	–0.33	5.78e–24
	PIK-93	–0.33	7.09e–24
	XMD13-2	–0.33	1.60e–23
	PHA-793887	–0.33	4.12e–23
	Vorinostat	–0.32	4.09e–20
	YM201636	–0.31	1.18e–20
CTRP			
EZH2	GSK-J4	–0.65	0.00e+0
	Necrosulfonamide	–0.45	2.16e–25
	Belinostat	–0.44	4.60e–18
	Teniposide	–0.43	3.47e–18

	Tozasertib	–0.43	3.27e–3
	PX-12	–0.43	5.82e–33
	BRD-K01737880	–0.42	0.01
	BRD-K30748066	–0.41	0.01
	sotrastaurin	–0.41	6.94e–21
	PRIMA-1	–0.40	6.19e–27

Supplementary Figure 1

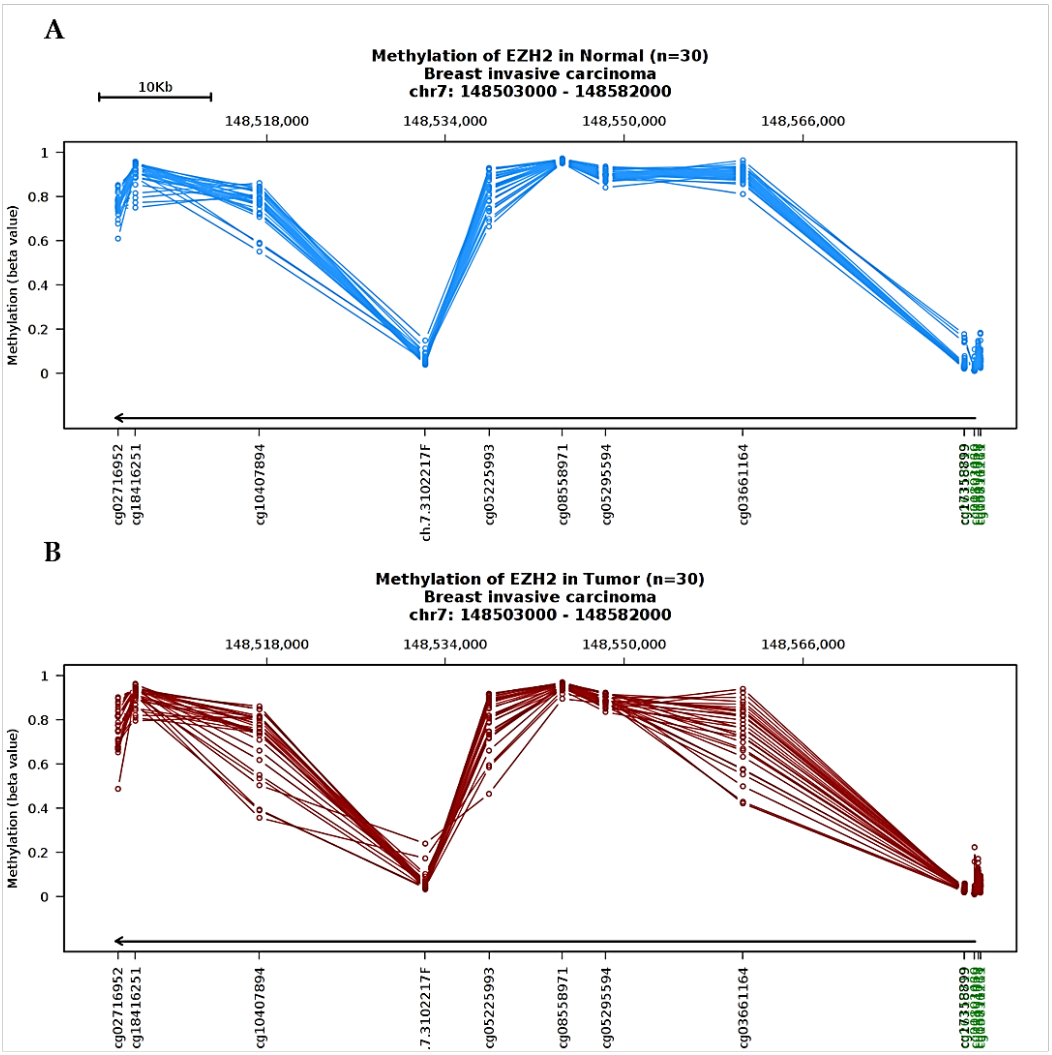

Supplementary Figure 2

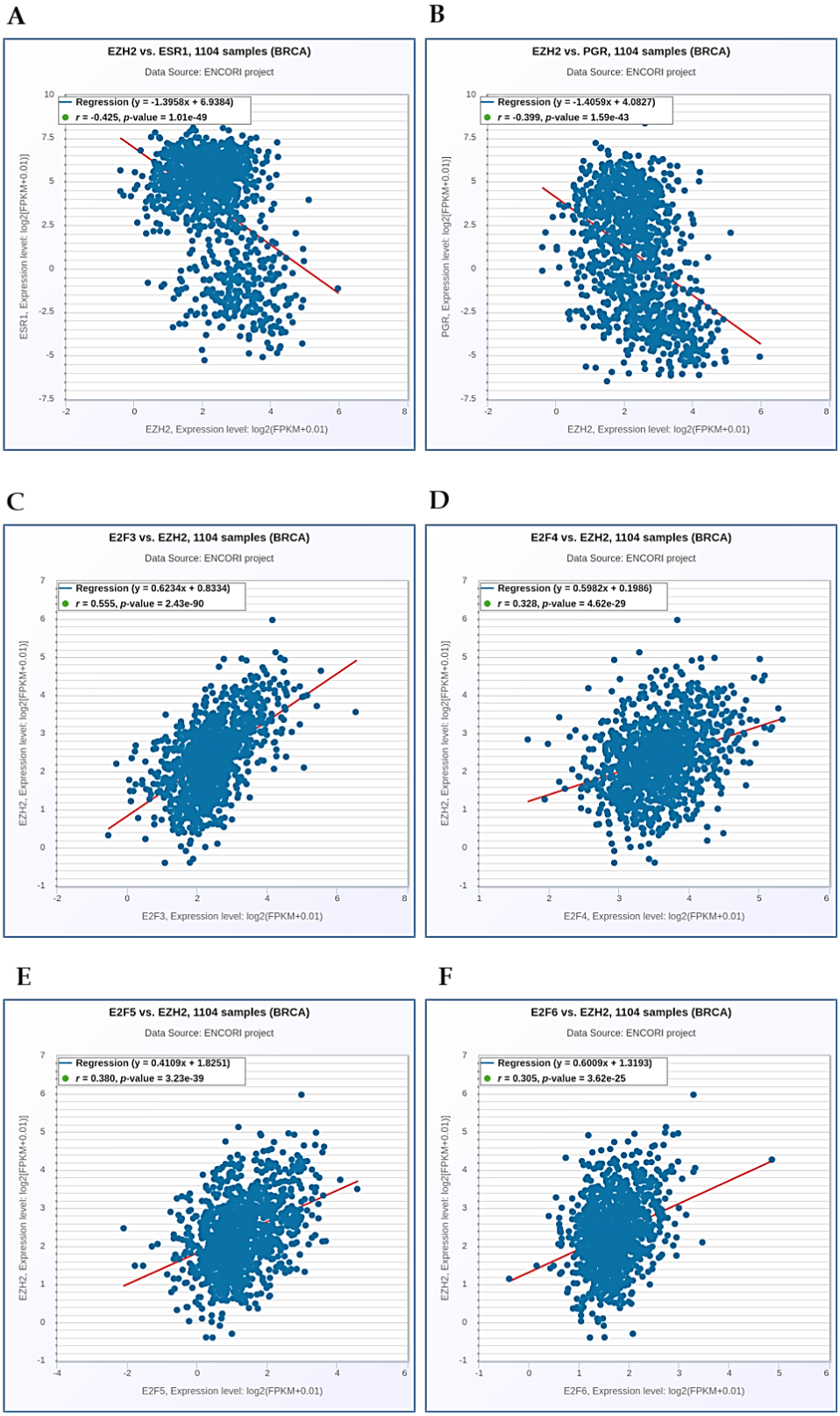

Supplementary Figure 3

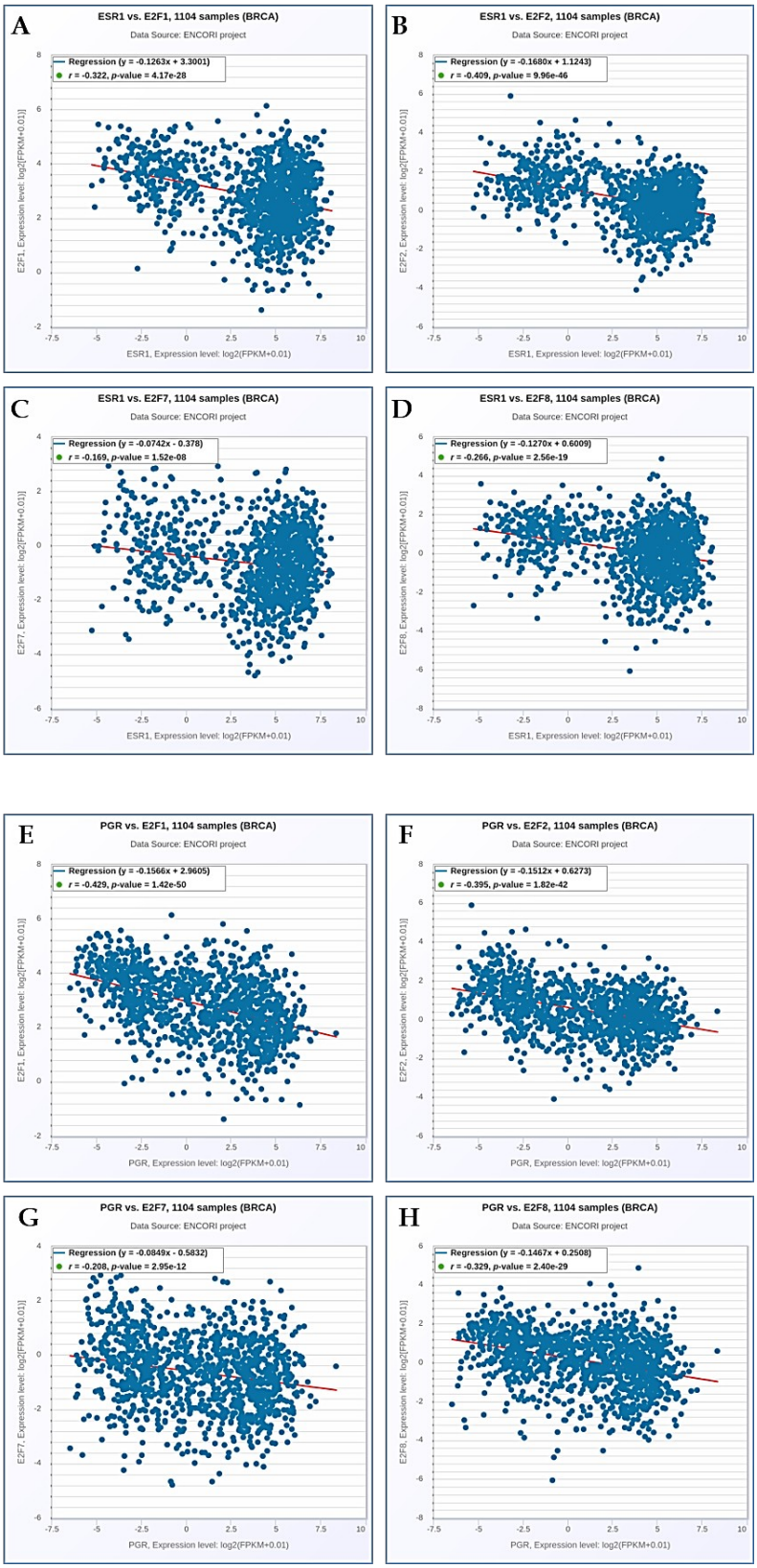

Supplementary Figure 4

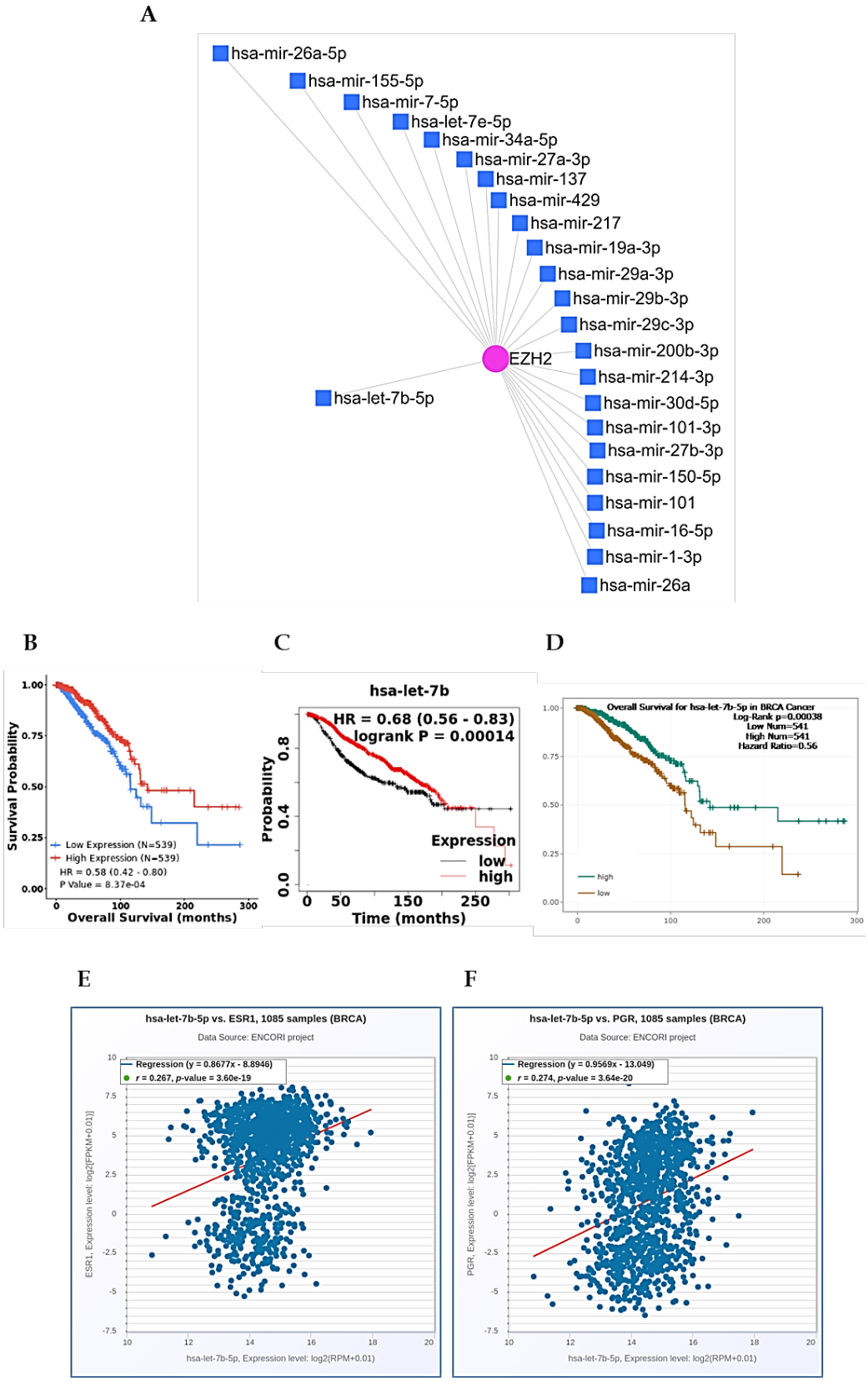

Supplementary Figure 5

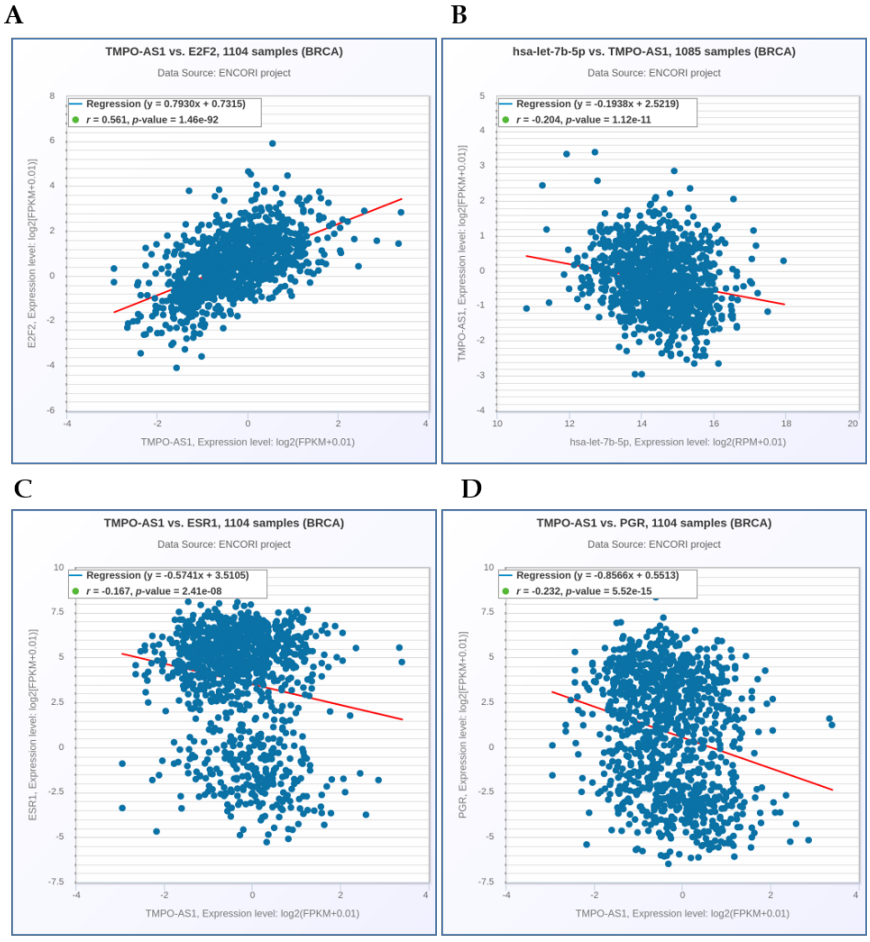
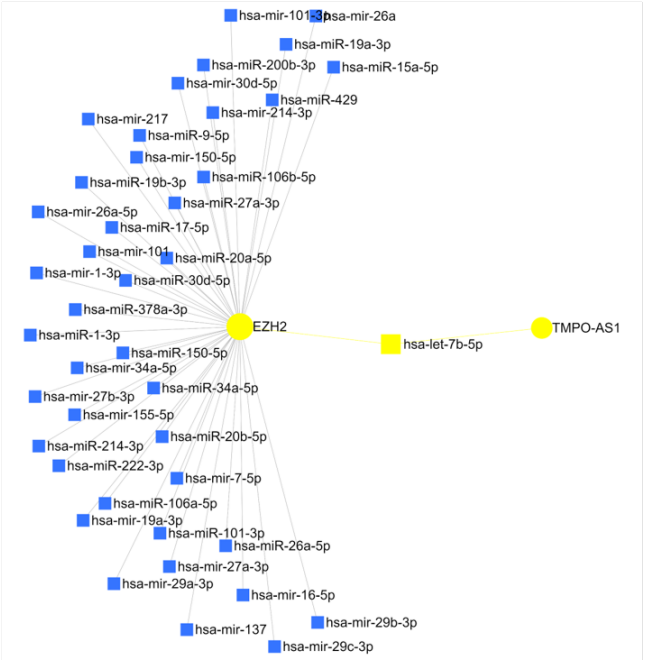
E